



DEMOCRATIC AND POPULAR ALGERIAN REPUBLIC
MINISTRY OF HIGHER EDUCATION AND SCIENTIFIC
RESEARCH



Université Kasdi Merbah-Ouargla

Kasdi Merbah-Ouargla University

Faculty of Hydrocarbons, Renewable Energy and Earth and Universe Science

Department of Hydrocarbon Production

Master dissertation

To obtain the Master's Degree

Option: Academic Production

Presented by

BOUAZZA SAFA

-THEME-

**NEW MESOFLUIDIC SYSTEM DESIGNED TO STUDY THE EFFECT
OF SNAP-OFF ON DISPLACEMENT. FLUID/FLUID AND
REMEDICATION BY STEAM INJECTION**

Publicly defended on: 06/16/2025 before the examination committee

Jury:

President	GHALI AHMED	SLB	Ouargla. Univ
Examiner	MEHASSOUEL Ammar	SLA	Ouargla. Univ
Rapporteur	BOUFADES Djamila	SLA	Ouargla. Univ
Co-Rapporteur	ADJOU Zakaria	Ph. D	Ouargla. Univ

Academic Year: 2024/2025

Acknowledgments

Our thanks first and foremost to ALLAH who granted us all the health, strength, and patience to accomplish our work.

*First of all, this work would not be as rich, nor would it have come to fruition without the help Precious help from **Dr. BOUAFDES Djamila** and **Dr. ADJOU Zakaria**, we thank them for the quality of their exceptional guidance and their rigor in successfully preparing this thesis. We had the honor of being among your students and benefiting from your teaching. We thank you infinitely for your hospitality and your advice. Please find here the expression of our gratitude and esteem.*

*We thank the jury members, **Dr. GHALI Ahmed** and **Dr. MEHASSOUEL Ammar** for the honor of accepting to evaluate this work. We also thank you for your attentive and highly relevant review of the entire thesis. This undoubtedly provides us with clarifications on important points, and we must pay more attention to it to guide our reflections in future research work.*

Our thanks also go to all our professors in the Production department as well as the administrative team for their generosity and the great patience they have shown. Our deepest thanks also go to all the people who have helped and supported us, near and far.

Dedication

First and foremost, to God, for the strength and countless blessings that made this achievement possible. to my beloved parents (Mebarki Djamila. Rabie), whose unwavering love, boundless patience, and endless encouragement were the bedrock of my strength throughout this journey to my aunt (Fatima) whos stand with in the defficult moment and encourage me thank you my dear, to my inspiring teachers, your passion for and your continuous encouragement were the driving forces behind my academic pursuits. I am thankful

To my dear siblings Moussaab, Aya, Bachir, Touba, Salah and Moudou whose accompanied me and shared with me the moments of joy, fun and sadness in life, I am very lucky to have you, to all the laboratory Workers who were by our side during the preparation of the memorandum(Bennouh Ferial ,Maarouf Nevin Anfel,Moulate bahemed ,Gummou Manar)

To myself – for the late nights, For the times I doubted but continued anyway, for the challenges I faced and overcame.

BOUAZZA Safa

Abstract

ملخص

الوسط الشعري هو بيئة معقدة للغاية تحتوي على العديد من المعلمات البتروفيزيائية وكذلك الظواهر اللزجة والشعيرية، ومن بين هذه الظواهر، فإن ظاهرة الانفصال المفاجئ لها تأثير كبير على احتجاز الأطوار المائية والزيتية أثناء تحولات النفط والماء على مقياس المسام. العمل يعتمد على تصميم نظام (mesofluidic) محب للزيت جديد بالإضافة إلى نظام خنق يعتمد على الحقن. تشمل الاختبارات التي تم إجراؤها الامتصاص، التصريف، الإزاحة المتزامنة للزيت/الماء مع تصور الانفصال. بعد ذلك، تم إجراء محاولة لحقن البخار من أجل تحريك المرحلة السائلة المحبوسة. تظهر نتائج العمل احتجاز الماء في الشعيرات الدموية ذات القطر الصغير بمعدل استرداد النفط بين 47% و 71%، بينما تتراوح نسبة الماء المنتج بين 91% و 97%. زمن الانفصال هو $3 \cdot 10^{-3}$ ثانية. تسمح هذه النتائج بفهم أفضل لسلوك الصخور الخزانية على المقياس المجهرى.

الكلمات المفتاحية : نظام الميسوفلويديك، السحب، التصريف، الامتصاص، عامل الاسترداد، حقن البخار.

Résumé

Le milieu capillaire est un milieu fortement complexe qui présente plusieurs paramètres pétrophysiques ainsi que des phénomènes visqueux et capillaires, dont le phénomène de snap-off a un impact important sur le piégeage des phases aqueuses et huileuses au cours des déplacements huile-eau à l'échelle des pores . Le travail est basé sur la conception d'un nouveau système mésosfluidiques oléophile ainsi un système d'étrangement à base des seringues. Les tests réalisés comprennent l'imbibition, le drainage, déplacement simultané huile/eau tout en visualisant le snap-off. Ensuite, une tentative d'injection de vapeur à été appliquée afin de mobiliser la phase fluide piégée. Les résultats du travail montrent le piégeage de l'eau dans les capillaires de petit diamètre avec un taux de récupération d'huile entre 47% et 71%, pour le pourcentage d'eau produite est compris entre 91% et 97%. Le temps de snap-off est de $3 \cdot 10^{-4}$ s. Ces résultats permettent de mieux comprendre le comportement des roches réservoir à l'échelle microscopique.

Mots clés : Système mésosfluidique, sanp-off, drainage, imbibition, facteur de récupération, injection de vapeur.

Abstract

The capillary medium is a highly complex environment that presents several petrophysical parameters as well as viscous and capillary phenomena, among which the snap-off phenomenon has a significant impact on the trapping of aqueous and oily phases during oil-water displacements at the pore scale. The work is based on the design of a new oleophilic mesofluidic system as well as a strangulation system based on syringes. The tests conducted include imbibition, drainage, simultaneous oil/water displacement while visualizing the snap-off. Next, an attempt to inject steam was made in order to mobilize the trapped fluid phase. The results of the work show the trapping of water in small-diameter capillaries with an oil recovery rate between 47% and 71%, while the percentage of water produced is between 91% and 97%. The snap-off time is $3 \cdot 10^{-4}$ s. These results allow for a better understanding of the behavior of reservoir rocks at the microscopic scale.

Key words: Mesofluidic system, sanp-off, drainage, imbibition, recovery factor, steam injection.

Table of Contents

Acknowledgments	II
Dedication	III
Abstract	IV
Table of Contents	VI
<i>List of figures</i>	VIII
List of tables	X
List of abbreviations	XI
GENERAL INTRODUCTION	1
Chapter I: Porous media characterization and capillary phenomenon	
Introduction	4
I.1 Multiphase flow in porous media	4
I.2 Static petrophysical properties:	5
I.2.1 Porosity	5
I.2.2 Capillary pressure	7
I.2.3 interfacial tension:	10
I.2.4 Wettability:	10
I.2.5 Saturation:	11
I.3 Dynamic petrophysical properties	13
I.3.1 Permeability	13
I.4 Preferential flow path	14
I.5 capillary phenomenon	15
I.5.1 Jamin Effect	15
I.5.2 Watter bypass	15
I.6 Snap off phenomenon	16
I.6.1 Definition:	16
I.6.2 Mechanisms of Snap-Off	17
I.6.3 Influencing Factors of Snap-Off	18
I.6.4 Steam injection	20
Conclusion	21

Chapter II Experimental strategy and laboratory protocol

Introduction	23
II.1 Materials used	23
II.1.1 Brine	23
II.1.2 Diesel	23
II.1.3 Crude oil	24
II.1.4 Wettability determination	25
II.1.5 Description of the mesofluidic system	26
II.2 Experimental procedures:	26
II.2.1 Drainage	27
II.2.2 Imbibition :	29
II.2.3 Simultaneous injection	31
II.3 Steam injection on PVC-mesofluidic system experiment	32
II.3.1 Description of the experiment	32
II.3.2 Material used on steam injection	32
II.3.3 Experimental procedure	33
Conclusion:	34

Chapter III: Results and discussion

Introduction	37
III.1 Oil properties results	37
III.2 Contact angle measurements results:	38
III.3 Preferential flow path during drainage process on mesofluidic system results	39
III.4 Snap off during imbibition process	42
III.5 Simultaneous injection	43
III.6 Visualization of Snap-off phenomenon	44
III.6.1 Observation and interpretation	46
III.6.2 Numerical application	46
III.7 Steam injection on mesofluidic system results	47
Conclusion:	49
General Conclusion and Recommendations	51
References	54
Appendix	57

List of figures

Figure I.1: conceptual representation of different types of pores in a reservoir rock.....	6
Figure I.2:porosity types	6
Figure I.3:Pressure relations in capillary tubes for an air–liquid system.....	7
Figure I.4:Dependence of capillary pressure on wetting characteristics and pore size	8
Figure I.5:initial saturation zones	9
Figure I.6:Capillary pressure drainage and imbibition curves.....	9
Figure I.7:Illustration of surface tension.....	10
Figure I.8:Contact angle on solid surfaces.....	10
Figure I.9:wettability types	11
Figure I.10:Fluid saturation distribution in a hypothetical reservoir rock sample [5].....	12
Figure I.11:darcy law	13
Figure I.12trapping of a droplet in a capillary tube	15
Figure I.13 the drainage, imbibition mechanisms for the pore doublet model.....	16
Figure I.14:Geometric Criteria for the Snap-Off of a Non-Wetting Droplet in Pore-Throat Channels With size	17
Figure I.15:Two typical snap-off processes. (a) Formation of a new gas bubble through snap-off. (b) Division of a long gas bubble into two smaller ones through snap-off.	17
Figure I.16:Snap-off-induced emulsions in a 3D pore–throat micromodel with triangular cross-sections	18
Figure I.17:Relationship between the capillary number and snap-off time using the BD model	18
Figure I.18:Two-phase flow behaviors within pore–throat connections with different length-to-diameter ratios.....	20
Figure II.1: Rotary viscometere instrument.....	24
Figure II.2: Steps of mesure surface and interfacial tension.....	25
Figure II.3: Contact angle determination imaging.....	26
Figure II.4: Schematic representation of the mesofluidic system apparatus	26
Figure II.5: Saturation of the system with oil	27
Figure II.6: Preferential flow path results under $p=0.00387$	28
Figure II.7: Preferential flow path results under $p= 0.00775$ atm.....	28

Figure II.8: Preferential flow path results under $p= 0.01549$ atm.....	28
Figure II.9: Preferential flow path results under $p= 0.01936$ atm.....	29
Figure II.10: Saturation of the system with water	30
Figure II.11: snap off phenomenon during imbibition proces	31
Figure II.12: simultaneous injection	32
Figure II.13: A) Steam injection experiment installation B) Schematic representation of the Steam injection installation.....	34
Figure III.1: final results of rotary viscometer.....	37
Figure III.2: graph displays a force (weight) versus time curves	38
Figure III.3: Contact angle between: (A) oil drop and glass plate(B) water drop and glass plate.....	39
Figure III.4: Preferential flow path results and Recovered oil under $p=0.00387$	40
Figure III.5 : Preferential flow path results and Recovered oil under $p= 0.00775$ atm	40
Figure III.6: Preferential flow path results and Recoverd oil under $p= 0.01549$ atm.....	41
Figure III.7: Preferential flow path results and Recoverd oil under $p= 0.01936$ atm.....	41
Figure III.8: snap off phenomenon during imbibition proces.....	43
Figure III.9: snap off phenomenon during simultaneous injection.....	44
Figure III.10: Photographs showing the occurrence of Snap-off phenomena.	44
Figure III.11: Dispersion of water droplets in oil	45
Figure III.12: Lamella formation and water droplet trapping.....	45
Figure III.13: Snap-off of a non-wetting phase droplet	45
Figure III.14: Formation of a film around the inner surface.....	46
Figure III.15: Observation of Snap-off phenomena using Vegas Pro 11.0.	47
Figure III.16: Residual oil recovered by steam injection in function of mesofluidic system temperature.	49

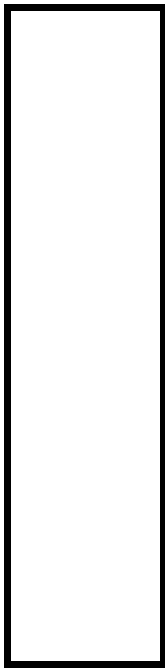
List of tables

Table 1: The range of porosity value with the type of sediment material	5
Table 2: Porosity and Permeability values for Reservoirs Qualitative Description	14
Table II-1: Properties of the diesel used	23
Table III-1: oil parameter.....	38
Table III-3: Oil recovery results	39
Table III-4: water recovery results.....	42
Table III-5: Heat energy transferred results.....	47
Table III-6: Residual oil recovered by steam injection's temperature ranges	48

List of abbreviations

$^{\circ}\text{C}$	Degree Celsius
atm	Atmosphere (Pressure unit)
BD model	Break-up Dynamics Model
Ca	Capillary Number
CSS	Cyclic Steam Stimulation
EOR	Enhanced Oil Recovery
g/cm^3	Gram per cubic centimeter
IFT	Interfacial Tension
k_{eff}	Effective Permeability
k_r	Relative Permeability
μ	Dynamic Viscosity
μ_p	Viscosity of Phase p
Pa	Pascal
P_c	Capillary Pressure
P_{cgo}	Gas-Oil Capillary Pressure
P_{cgw}	Gas-Water Capillary Pressure
P_{cwo}	Water-Oil Capillary Pressure
PVC	Polyvinyl Chloride
Q_p	Flow Rate of Phase p
RF	Recovery Factor
σ	Surface or Interfacial Tension
σ_{ij}	Interfacial Tension between Phase i and j
σ_{so}	Solid-Oil Interfacial Tension
σ_{sw}	Solid-Water Interfacial Tension
σ_{wo}	Water-Oil Interfacial Tension
S_f	Fluid Saturation

Shc	Hydrocarbon Saturation
SLB	Schlumberger
Sorg	Residual Oil Saturation (Gas-oil)
Sorw	Residual Oil Saturation (Water-oil)
So	Oil Saturation
Soc	Critical Oil Saturation
Sw	Water Saturation
Swc	Connate Water Saturation
Swirr	Irreducible Water Saturation
TEOR	Thermal Enhanced Oil Recovery
t _b	Break-up Time
τ _s	Snap-off Time
V	Volume
ΔP	Differential Pressure
∇P _p	Pressure Gradient of Phase p



General introduction

GENERAL INTRODUCTION

Prior research has shown that the lithologic characteristics of rocks affect their reservoir characteristics, including surface area, irreducible water saturation, permeability, and porosity. One particular rock feature has the same amount of influence on various reservoir rock types because of these variations. This relationship implies that there is some risk involved in attempting to define a reservoir purely on the basis of easily accessible variables, like permeability or grain shape. Cementation can mask their importance with sorting and other factors. Understanding the geology of the reservoir rock types and being able to spot changes within them are essential for making accurate fluid flow predictions [01].

Displacement processes one of the most significant trapping mechanisms is the snap-off phenomenon, where the wetting phase pinches droplets of the non-wetting phase in narrow pore throats. This process creates discontinuous globules of hydrocarbons that become immobile [02].

Hypotheses

The study is predicated on a number of important hypotheses:

1. Fluid flow dynamics and oil recovery efficiency are greatly influenced by the snap-off phenomenon both for oil and water phases.
2. By decreasing oil viscosity and changing fluid interactions within the pore spaces, thermal enhanced oil recovery techniques—specifically steam injection—improve oil mobility and recovery efficiency.
3. Variations in wettability and saturation levels within porous media have a significant impact on the efficiency of oil displacement by injected water or steam, and mesofluidic systems can faithfully replicate the behavior of dual phase flow in actual reservoir conditions, offering important insights into fluid dynamics and displacement patterns.

Problematic of the study

This work primarily addresses the issue of how water-oil displacement and hydrocarbon recovery rates in capillary media are affected by pore distribution and connectivity, which is influenced by variables like system wettability. Furthermore, using real-time visualization and sophisticated experimental simulation techniques through new designed mesofluidic system, it investigates whether thermal recovery techniques can successfully address these issues to improve overall recovery efficiency.

Objectives of the study

This work's primary goals are:

- 1- providing basic concepts to build a strong foundation for full understanding of the study
- 2- studying and observing the snap-off phenomenon and its impact on two-phase flow using mesofluidic system
- 3- steam injection as a solution of this trapping and evaluate the efficacy of it
- 4- taking real data from an oil field and simulating it with CMG simulator

Organization of the dissertation

The structure of the manuscript is as follows:

The first chapter includes the main basic concepts of multiphase flow in porous medium, static and dynamic petrophysical properties of the reservoir rocks. Also, the snap-off phenomenon, its mechanism, main factors influence oil/water retention in the capillary system and its impact on oil and water displacement.

The second chapter outlines the experimental methodology and steps for using a new designed mesofluidic system to study two-phase water-oil flow in capillary media. Real-time visualization of snap-off phenomenon at the pore scale is made possible by mesofluidic technique based on PVC system. In order to better understand fluid behavior and optimize recovery strategies, the chapter includes thermal recovery experiments to assess the effects of heat-based methods on oil recovery.

The third chapter evaluates the efficiency of heat recovery techniques and talks about the creation of preferential flow paths. Oil recovery strategy optimization snap-off effect, which offer deeper insights into fluid displacement mechanisms and water-oil displacement.

Finally, a conclusion and recommendations are listed to overcome future negative impacts of capillary phenomena and support the application of thermal enhanced oil recovery.



Chapter I

Porous media characterization and capillary phenomenon

Introduction

In the intricate realm of multiphase flow through porous media, a phenomenon of critical importance is snap-off. This process, fundamentally driven by interfacial instabilities and capillary forces, leads to the detachment of a continuous non-wetting fluid into discrete droplets or bubbles within the pore network. In this chapter we will mention several fundamental concepts: flow types, petrophysics parameters, snap-off phenomenon, and factors that affect it. we will explain every characteristic that has a relation to our subject for well understanding and simplifying our study as much as we can.

I.1 Multiphase flow in porous media

Multiphase flow through porous media is important for a various application such as enhanced oil recovery. These often involve the imbibition. Modeling of multiphase flow, on the other hand is still an enormous technical challenge.

It is assumed that the flow rate is proportional to the pressure gradient, governed by a Darcy-type law:

$$Q_p = \frac{K_{rp}k}{\mu_p} (\nabla P_p - \rho_p g) \quad (I;1)$$

Q_p : the volume of phase p flowing per unit area per unit time,

K_{rp} : the relative permeability,

K : the absolute permeability, μ_p is the viscosity,

∇P_p : the pressure gradient

$\rho_p g$: the contribution of gravity. [1]

Consider two immiscible fluids simultaneously present in a porous medium. Their equilibrium or motion is governed.

Both fluids are subject to viscous flow, which is almost always laminar. If the flow is assumed to be iso-thermic and the fluids Newtonian, such flows are mathematically described by Navier-Stokes equations:

$$\text{grad } P - \rho \text{ grad } g = (\lambda + \mu) \text{ grad } \text{div } \vec{v} - \rho \frac{d\vec{v}}{dt} \quad (I;2)$$

P = pressure

ρ = specific gravity,

$\text{grad } g$ = gravity acceleration vector,

$\text{grad } \text{div } \vec{v}$ = fluid velocity vector,

Chapter I: Porous media characterization and capillary phenomenon

$\frac{\vec{d}}{dt}$ = derivative with respect to time, following the fluid particle,

Δ = Laplacian operator,

Θ = speed of cubic expansion of the fluid $\Theta = \text{div } \vec{v}$

Λ and η viscosity coefficients. [2]

I.2 Static petrophysical properties:

I.2.1 Porosity

the rock reservoir is basically a result of sand grains of different sizes that produce pores, porous rock is the important feature of reservoirs, Porosity(\emptyset) could be the simplest reservoir rock property to understand and to use in reservoir studies including building reservoir simulation model. According to Tissot and Welte,1 most sedimentaries rocks have grain diameters in the range of 0.05–0.25 mm, resulting in average radii of the void spaces or pores or tiny openings between 20 and 200 μm . [1]

Table 1: The range of porosity value with the type of sediment material

Type of Sediment Material	3.1. Porosity (%)
Soil	50-60
Clay	45-55
Silt	40-50
Medium coarse sand	35-40
Sand	30-40
Medium fine sand	30-35
Gravel	30-40
Gravel and sand	20-30
Breccias	10-20
Flake	1-10
Limestone	3.2. 1-10

Porosity is a scalar dimensionless variable that tends to change in a linear manner. The porosity that was formed during rock deposition is known as the primary porosity. Additional porosity that was formed due to later geological events is considered a secondary porosity. It includes fractures in different rocks and solution cavities in carbonates [2] This significant reservoir rock property is denoted by (\emptyset) and is mathematically expressed by the following relationship:

$$\emptyset = \frac{\text{Pore volume}}{\text{Total or bulk volume}} \quad (\text{I;3})$$

Chapter I: Porous media characterization and capillary phenomenon

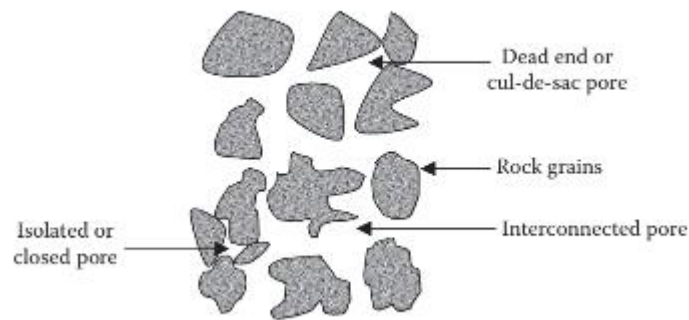


Figure I.1: conceptual representation of different types of pores in a reservoir rock

- Types of porosities:

- absolute porosity $\emptyset = \frac{\text{total pore volume}}{\text{total rock volume}}$ (I,4)

- effective porosity: $\emptyset = \frac{\text{Vol. of interconnected pores} + \text{Vol. of dead-end}}{\text{total volume}}$ (I,5)

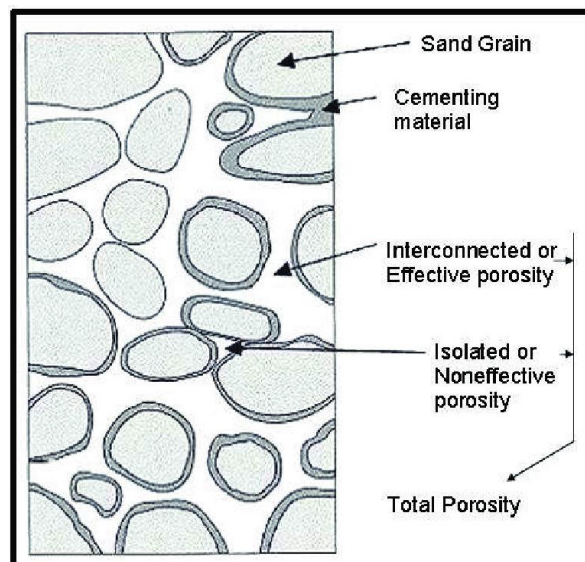


Figure I.2: porosity types

- Factors that affect porosity:
- Particle shape and size
- Type of Packing Cementing materials
- Overburden stress Fractures

I.2.2 Capillary pressure

The surface and interfacial tensions of the rock and fluids, the pore size and geometry, and the system's wetting properties all work together to produce the capillary forces in a petroleum reservoir [3]

P_c is the difference in pressure between two immiscible fluids across a curved interface at equilibrium. Curvature of the interface is the consequence of preferential wetting (adhesion properties) of the capillary walls to the fluid phases [4]

It is usually calculated as: $P_c = P_{nwt} - P_{wt}$ (I;6)

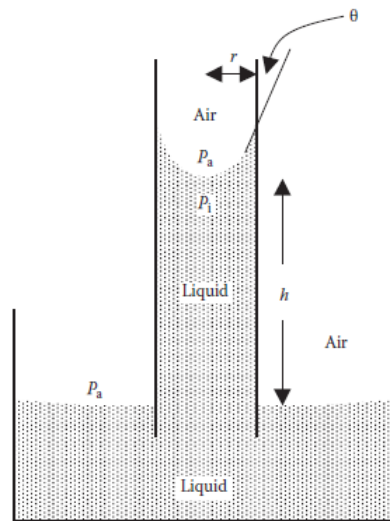


Figure I.3: Pressure relations in capillary tubes for an air–liquid system.

Pressure relations in capillary tubes for an air–liquid system.

There are three types of capillary pressure:

- P_{cwo} : Water-oil capillary pressure $p_{cwo} = p_o - p_w$ (I;7)

- P_{cgo} : Gas-oil capillary pressure $p_{cgo} = p_g - p_o$ (I;8)

- P_{cgw} : Gas-water capillary pressure $P_{cgw} = p_g - p_w$ (I;9)

In the case of a capillary tube of radius r containing oil and water, application of Laplace and Young's equation gives the relationship

$$P_c = \frac{2\delta \cdot \cos \theta}{r} \quad (\text{I;10})$$

there are several factors affect the capillary pressure:

IFT, contact angle, pores size, saturation and wetting properties.

Chapter I: Porous media characterization and capillary phenomenon

- Dependence of capillary pressure on rock and fluid properties

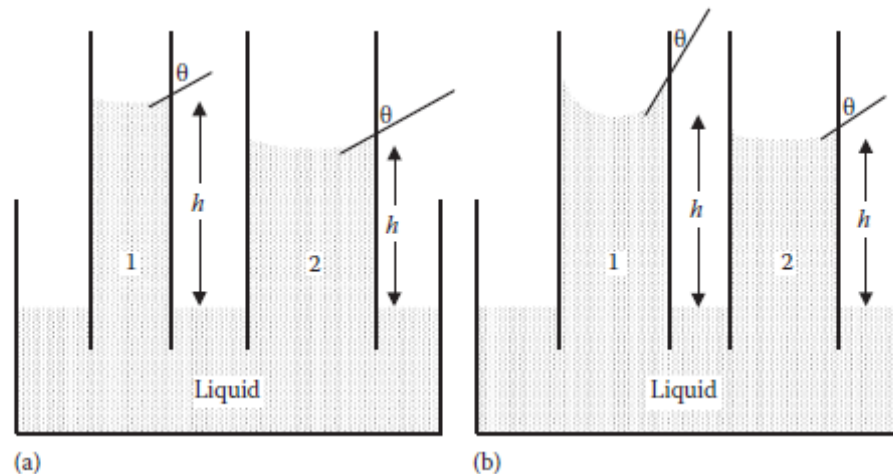


Figure I.4: Dependence of capillary pressure on wetting characteristics and pore size
Case (a): we have the same wetting characteristics (IFT, θ) and different radius size in this case, the capillary pressure is inversely proportional to the capillary.

the higher the capillary tube radius, the lower the capillary pressure [1]

Case (b): we have the same radius and different characteristics in this case value of capillary pressure will be directly proportional to the adhesion tension or the wetting characteristics of the system.

In this case, the smaller the contact angle, the greater the height of liquid rise and stronger the adhesion tension, leading to higher capillary pressure [1]

- Relation pression capillaries-saturation

Three saturation zones can be used to initially categorize the reservoir system. The first is the oil zone, where the only mobile phase at first is oil and the water saturation is constant at its lowest (S_{wir}) value. The second is the transition zone, when both water levels and saturation are rising with depth and oil are movable. The third is the water zone (aquifer), where only water is movable and water saturation is at its highest (100%) value. Well W-1 will initially produce water-free oil, well W-2 should be finished in the oil zone to prevent early water production, and well W-3 will most likely generate water with oil at first, according to the same figure [5]

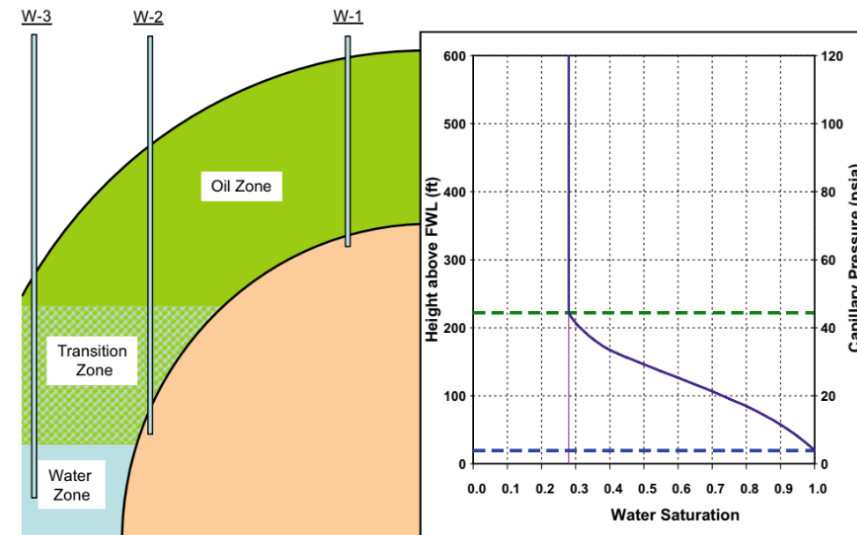


Figure I.5: initial saturation zones

- Drainage and Imbibition Capillary Pressure Curves

The process of fluid movement where the nonwetting phase becomes more saturated, displacing the wetting phase with a nonwetting phase, is what largely determines the fluid saturations detected when the reservoir is found.

The wetting phase is displaced until reaching some minimum irreducible saturation. This irreducible water saturation is referred to as connate water, S_{wc} . [5]

Imbibition.

The drainage process is reversed by replacing the nonwetting phase with the wetting phase in a fluid flow process where the saturation of the wetting phase rises. As wetting phase saturation rises, so does wetting phase mobility. [5]

This difference in the two capillary pressure curves (Drainage & Imbibition) is called capillary hysteresis [5]

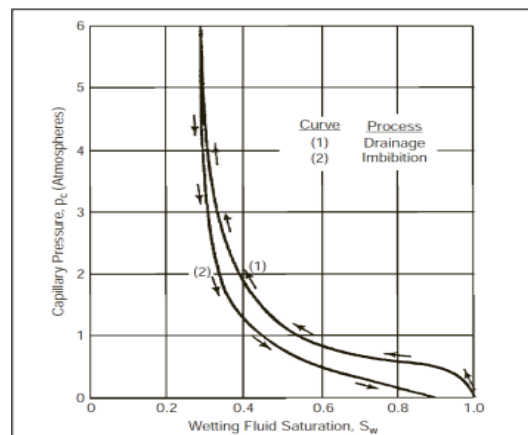


Figure I.6: Capillary pressure drainage and imbibition curves

I.2.3 interfacial tension:

In the broader sense, IFT is defined as the work which must be expended to increase the size of the interface between two adjacent phases which do not mix completely with one another. In the narrower sense the term relates to the liquid/liquid and liquid/solid phase boundaries, while for the liquid/gaseous interface we refer to surface tension and for the solid/gaseous interface we refer to surface free energy. [6]

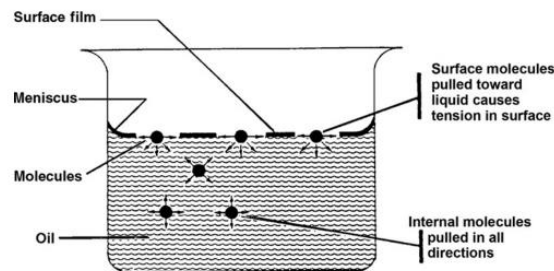


Figure I.7: Illustration of surface tension.

I.2.4 Wettability:

The inclination of one fluid to spread or stick to a solid surface when there are additional immiscible fluids present is known as wettability. The wetting phase in a two-phase system is the phase that has a tendency to stick to the solid rock surface. The non-wetting phase is the other phase. Compared to the non-wetting phase, the wetting phase is more difficult to move because it tends to occupy the smaller pores. [2]

- Contact angle and wetting

If a small drop of liquid is placed on a uniform flat solid surface it will, in general, not spread completely over the surface. However, its edge will make an angle θ with the solid. [7]

The angle between the tangent to the liquid surface at the point of contact and the solid surface inside the liquid is called contact angle for that liquid/solid combination. It strongly depends upon the nature of the liquid and the solid, and can have values between zero and π rad [7]

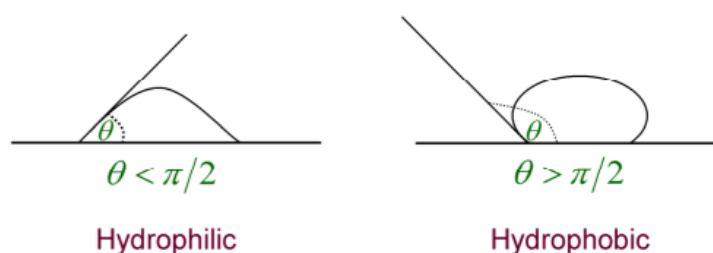


Figure I.8: Contact angle on solid surfaces

Chapter I: Porous media characterization and capillary phenomenon

-where two liquids(w/o) are associated with a solid surface, the contact angle is:

$$\cos\theta = \frac{\sigma_{so} - \sigma_{sw}}{\sigma_{wo}} \quad (I;11)$$

σ_{so} :interfacial tension between the solid and oil

σ_{sw} : interfacial tension between the solid and water

σ_{wo} :interfacial tension between water and oil

Types of Wettability

- Water Wet
- Oil Wet
- Intermediate Wet
- Fractional Wettability
- Mixed Wettability

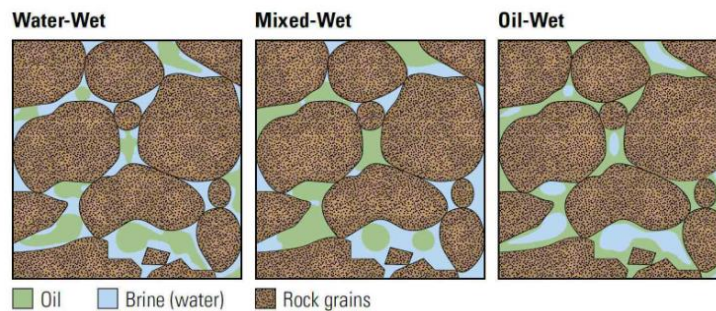


Figure I.9:wettability types

● Factors Affecting Reservoir Wettability

- Oil composition. And Rock mineralogy.
- Connate water composition and ph.
- Depth of the reservoir structure
- pressure and temperature of reservoir

I.2.5 Saturation:

- Definition:

Sf is defined as that fraction or percent of the pore volume occupied by a particular fluid phase it is a dimensionless scalar variable. It can be expressed as fraction or percentage, Fluid saturation is one of the essential parameters for estimating the hydrocarbon in place .[8]

$$Sf = \frac{vf}{vp} \quad (I;12)$$

- Case of gas $Sg = \frac{vg}{VP}e: \quad (I;13)$

Chapter I: Porous media characterization and capillary phenomenon

Case of water:
$$S_w = \frac{V_w}{V_p} \quad (\text{I};14)$$

Case of oil:
$$S_o = \frac{V_o}{V_p} \quad (\text{I};15)$$

$$S_o + S_g + S_w = 1 \quad S_{hc} = 1 - S_w \quad (\text{I};16)$$

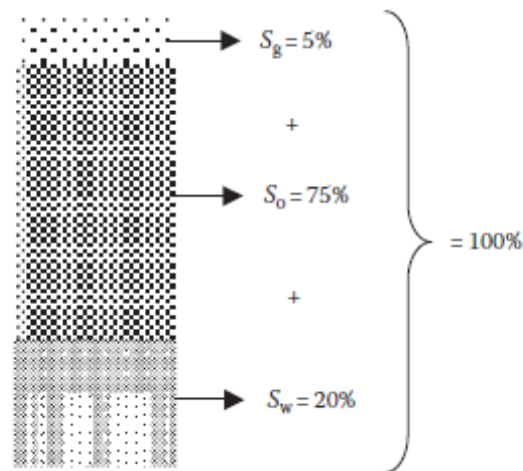


Figure I.10: Fluid saturation distribution in a hypothetical reservoir rock sample [5]

Irreducible water saturation (S_{wirr}):

Although it is often measured in a laboratory and is not always observed in a reservoir, irreducible water saturation (S_{wirr}) is the lowest value of water saturation that can exist in a reservoir system and is dependent on the condition of the rock. [2]

Residual Oil Saturation (S_{or}):

is the oil saturation at which the oil phase become immobile and it is the minimum possible oil saturation in the oil reservoir? This saturation is reached as result of complete displacement of oil from the pores. There are two different residual oil saturation, the water–oil residual oil saturation (S_{orw}) which reached by water displacing oil and the gas–oil residual saturation (S_{org}) caused by gas displacing oil. These residual oil saturations are the ones that can be achieved by primary drive forces and secondary recovery methods. Successful tertiary recovery methods would reduce the residual oil saturation and consequently increase ultimate oil recovery. We should be clear about the difference between residual oil saturation and remaining oil saturation. [2]

Critical oil saturation, S_{oc}

For the oil phase to flow, the saturation of the oil must exceed a certain value,

Chapter I: Porous media characterization and capillary phenomenon

which is termed critical oil saturation. At this particular saturation, the oil remains in the pores and, for all practical purposes, will not flow. [3]

I.3 Dynamic petrophysical properties

I.3.1 Permeability

Permeability is a property of the porous medium that measures the capacity and ability of the formation to transmit fluids. The rock permeability, K is a very important rock property because it controls the directional movement and the flow rate of the reservoir fluids in the formation. This rock characterization was first defined mathematically by Henry Darcy in 1856 [3]

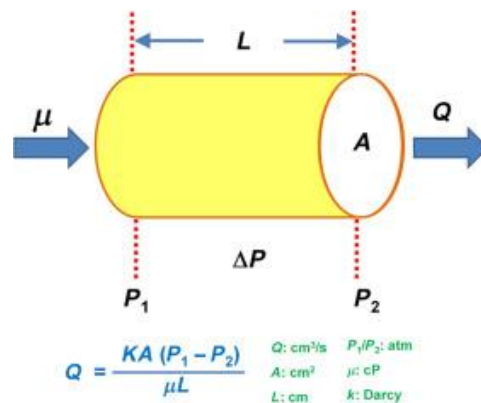


Figure I.11: darcy law

- absolute permeability k_a

Permeability (k) is a measure of the ease with which a porous medium will transmit fluid, whereas absolute permeability (k_a) is the measure of the ease of flow of a single fluid through the reservoir rock. It is an intrinsic reservoir rock property (i.e., fluid, and solid–fluid interactions do not influence k_a) that is independent of the type of fluid (gas, water, oil) provided the fluid occupies 100% of the conductive pore space. It is a function of pore size distribution only. Darcy's law presented in Eq. (I;17) is used to determine permeability (especially in macropores) under the following conditions : a laminar subsurface flow (non-turbulent), no reaction between rock and fluid, and one phase present at 100% pore space saturation

$$K_a = \frac{Q\mu\Delta L}{A\Delta P} \quad (\text{I;17}) \quad [10]$$

- Effective permeability k_{eff}

Effective permeability of rock to a fluid phase (oil, gas, or water) in porous medium is a measure of the ability of that phase to flow in the presence of other fluid phases. the effective

Chapter I: Porous media characterization and capillary phenomenon

permeability to a fluid phase is based upon the presence of two or three fluid phases in porous medium

It is dependent on fluid saturation [11]

- relative permeability K_r

is defined as the ratio of effective permeability to absolute permeability. Relative permeability shows the ability of a system for flowing fluid in the presence of other fluids. The range of this dimensionless parameter is between 0 and 1. The value and curvature of the relative permeability definitely depends on wettability of the rock.

relative permeability is given by the following equation:

$$K_{ri} = \frac{K_{eff}}{K_a} \quad (I;18) \quad [12]$$

Table 2: Porosity and Permeability values for Reservoirs Qualitative Description

Qualitative Evaluation of Porosity	
Percentage Porosity (%)	Qualitative Description
0 - 5	Negligible
5 - 10	Poor
15 - 20	Good
20 - 30	Very Good
> 30	Excellent
Qualitative Evaluation of Permeability	
Average K_v Value (md)	Qualitative Description
< 10.5	Poor to fair
15 - 50	Moderate
50 - 250	Good
250 - 1000	Very Good
> 1000	Excellent

I.4 Preferential flow path

preferential flow path refers to a localized pathway through which fluids move more rapidly compared to the others, due to higher connectivity which is depend on shape of chanel and the destribution of porosity (effective). it is allowed to quantify the increase in the path travelled by the fluids in the rock, there are several factors effect it: rock properties (porosity, wettability, heterogeneity) fluid properties (viscosity, contact angle, surface tention) this pathway result from structural heterogeneities and can influence fluid transport dynamics

I.5 capillary phenomenon

I.5.1 Jamin Effect

is defined as that resistance to liquid flow through capillaries which is due to the presence of bubbles. Presence of bubbles can retard the flow of a liquid as it progresses through a capillary tube of small diameter. The Jamin effect may be defined as that resistance to flow under pressure through a capillary tube which is encountered by liquid globules interspaced with large bubbles. This effect or action is a phenomenon quite apart from frictional resistance and is due to difference of capillary pressure between two sides of the trapped globule. This effect can be described more easily by analyzing a trapped oil droplet or gas bubble in a preferentially water wet capillary tube. [3]

In Figure 01 assume the system is static with different pressure existence between point A and B because of capillary forces. The static pressure difference must be exceeded for flow to occur, in other words the static pressure difference, $P_A - P_B$, must be overcome to initiate flow. [3]

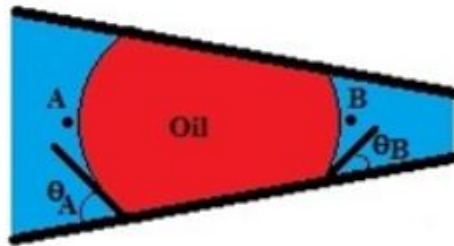


Figure I.12 trapping of a droplet in a capillary tube

Trapping of a Droplet in a Capillary Tube

$$P_a + \left(\frac{2\sigma_{ow}\cos\theta}{r}\right)_a - \left(\frac{2\sigma_{ow}\cos\theta}{r}\right)_b = P_b \quad (I;19)$$

$$P_b - P_a = 2\sigma_{ow}\cos\theta \left(\frac{1}{r_a} - \frac{1}{r_b}\right) \quad (I;20) \quad [3]$$

I.5.2 Water bypass

the non-wetting phase tends to invade the larger pores because of the lower capillary pressure. This tendency leads to special trapping mechanism named bypassing. The main trapping mechanism in drainage is bypassing although during the imbibition process non-wetting phase could be trapped by bypassing mechanism but it is not the major trapping mechanism.

Chapter I: Porous media characterization and capillary phenomenon

A reservoir rock consists of a complex network of branching and reuniting pore elements of differing sizes and geometry. Any successful analysis of the displacement process should eventually recognize this complex network. However, one can begin by understanding the processes which take place in the simpler elements of the network. The mechanisms of drainage displacement and imbibition displacement are best illustrated by visualization of flow experiments in transparent capillary networks etched on glass plates. The simplest type of pore system used in such displacement studies is the pore doublet. [4]

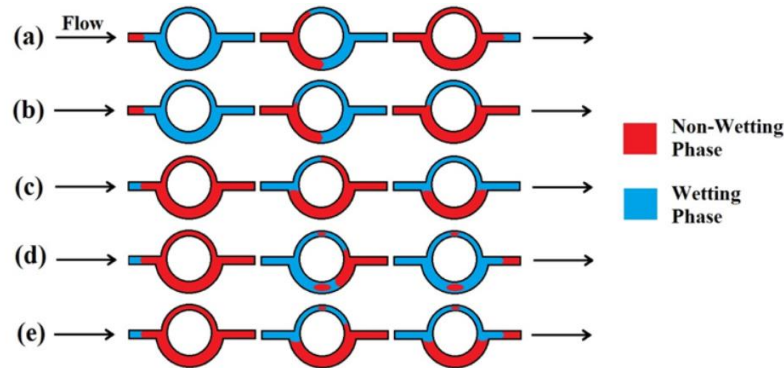


Figure I.13 the drainage, imbibition mechanisms for the pore doublet model

- (a) Drainage Process, No Trapping
- (b) Drainage Process, Bypassing in Smaller Throat
- (c) Imbibition Process, Bypassing in Larger Throat
- (d) Imbibition Process, Snap-Off
- (e) Imbibition Process, Snap-Off in Smaller Throat and Bypassing in Larger Throat. [4]

illustrates the drainage and imbibition mechanisms for the pore doublet model.

I.6 Snap off phenomenon

I.6.1 Definition:

snap-off, choke-off, or breakup is the breakup of the non-wetting fluid into separate droplets/bubbles because of the displacement of a nonwetting fluid by a wetting fluid in a pore-throat channel. This phenomenon occurs when the capillary pressure at its leading part exceeds that at the pore-throat junction during the imbibition process. It is an important process in many subsurface engineering applications, such as aquifer remediation, carbon capture and geological storage, and recovery of hydrocarbons [12]

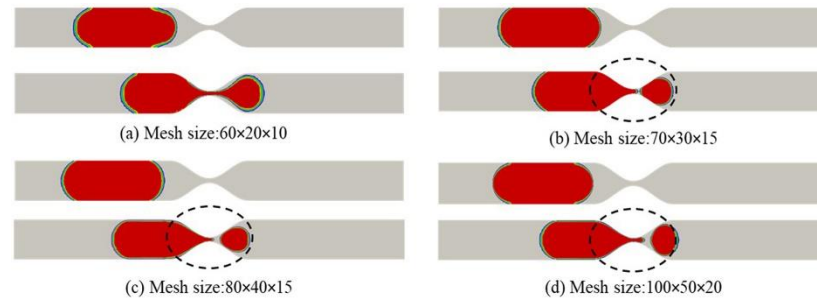


Figure I.14: Geometric Criteria for the Snap-Off of a Non-Wetting Droplet in Pore-Throat Channels With size

I.6.2 Mechanisms of Snap-Off

The occurrence of snap-off was initially noted during investigations of fluid transport within porous media in the early 1960s. This phenomenon encompasses the snap-off of gas bubbles in the presence of water, as well as the snap-off of oil droplets in the context of oil–water coexistence. [14]

Roof observed oil droplets formed through snap-off during waterflooding experiments in 1970. In this experiment (fig I.15), glass tubing with circular cross-sectional pore–throat structures were utilized to replicate the waterflooding process within water-wet media, and the snap-off phenomenon was observed [14]

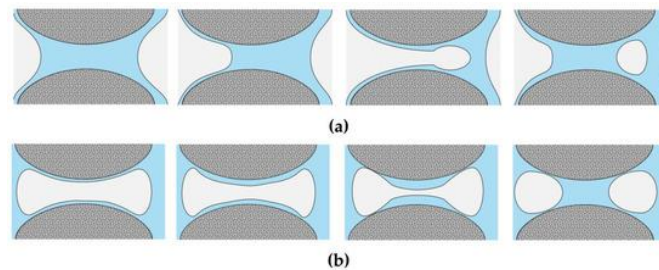


Figure I.15: Two typical snap-off processes. (a) Formation of a new gas bubble through snap-off.

(b) Division of a long gas bubble into two smaller ones through snap-off.

Based on these early experimental studies, the mechanisms underlying snap-off encompass variations in the curvature radius of the two-phase fluid interface within confined regions and the impact of capillary pressure. These mechanisms give rise to the instability of the collar-shaped interface of the two-phase fluids, ultimately resulting in the occurrence of the snap-off phenomenon within the narrow constriction. [14]

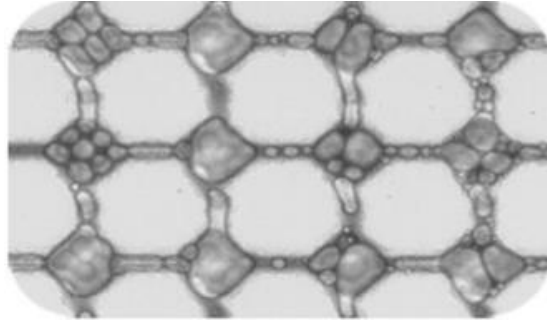


Figure I.16: Snap-off-induced emulsions in a 3D pore-throat micromodel with triangular cross-sections

I.6.3 Influencing Factors of Snap-Off

- The capillary number

(Ca) is a dimensionless number used to describe the flow behavior of fluids within capillaries or small channels. It is defined as Equation [2],

$$Ca = \frac{\mu V}{\sigma_{ij}} \quad (I;21)$$

μ = viscosity of the wetting phase

V = characteristic shear rate

σ_{ij} = interfacial tension [14]

The snap-off phenomenon occurs within a specific range of capillary numbers. Tsai and Miksis investigated how snap-off was affected by the capillary number. Using simulation methods, they determined two critical values of the capillary number that indicate when snap-off occurs. If the actual capillary number falls within the range defined by the first and second critical values, snap-off can occur more rapidly. When the actual capillary number was below this transitional threshold, the formation time of snap-off demonstrated a direct proportionality to the capillary number. Deng et al. utilized the BD model to investigate the impact of dynamic factors on snap-off in constricted capillary tubes and calculated the required time for snap-off. [15]

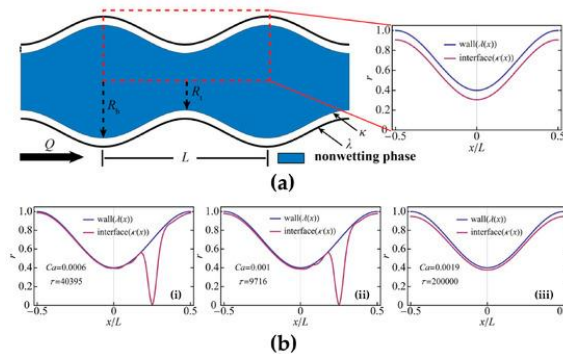


Figure I.17: Relationship between the capillary number and snap-off time using the BD model

Chapter I: Porous media characterization and capillary phenomenon

- (a) Schematic representation of the single-pore geometry in the simulation;
- (b) Corresponding required snap-off formation time at different capillary numbers demonstrate the inhibition of snap-off occurrence with capillary numbers of 0.0006, 0.001 and 0.0019, respectively, reprinted from Ref

- Viscosity Ratio and flow Rate Ratio

When both wetting and nonwetting phases coexist within a porous medium, their viscosity ratio, denoted as the wetting–nonwetting viscosity ratio $\gamma = \frac{\mu_w}{\mu_{nw}}$

variations in the viscosity ratio exert a direct influence on the interactions between the wetting and nonwetting phases, profoundly affecting the occurrence of snap-off and the ensuing behaviors at their interfaces.

The flow rate ratio, significantly influence the size, quantity, distribution, and stability of droplets formed during the snap-off process. Generally, a rise in the flow rate ratio results in snap-off droplets with smaller dimensions, a higher quantity of droplets, uneven spatial distribution, and reduced stability [16]

- Wettability of Porous Media

intermediate wettability of the media, while reducing the occurrence of pronounced snap-off phenomena, results in a more even distribution of oil and water within such media. This, in turn, can lead to less-efficient displacement of crude oil. it is essential to recognize that intermediate wettability of the media, while reducing the occurrence of pronounced snap-off phenomena, results in a more even distribution of oil and water within such media. This, in turn, can lead to less-efficient displacement of crude oil. [14]

Pore–Throat Connection. conducted experiments using microfluidic pore–throat systems in which they systematically varied the length-to-diameter ratio during oil–water imbibition experiments to analyze the impact of pore–throat connections on snap-off phenomena. The experimental results demonstrated that, under different length-to-diameter ratios, distinct displacement behaviors occurred, as depicted in Figure 8. Specifically, when the length-to-diameter ratio was less than π , piston-like displacement dominated as the primary mode during imbibition. Despite the nonwetting phase still being located at the pore–throat center due to wettability effects, it collectively moved forward as it was displaced by the wetting phase. Conversely, when the length-to-diameter ratio equaled or exceeded π , the snap-off phenomenon became nearly inevitable. This implies that the geometric dimensions of the pore–throat can reliably serve as a determinant for evaluating the likelihood of snap-off occurrence. These research findings align with the Rayleigh–

Chapter I: Porous media characterization and capillary phenomenon

Plateau instability theory underscores the direct influence of pore–throat geometric characteristics on snap-off occurrences. Moreover, it is noteworthy that for porous media with noncircular cross-sections, the hydraulic diameter can serve as a suitable proxy for the diameter when applying the Rayleigh–Plateau instability theory to assess the potential for snap-off. [16]

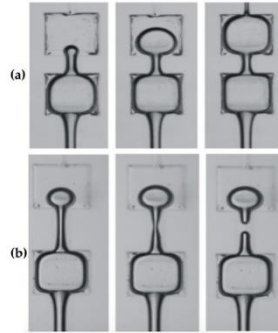


Figure I.18: Two-phase flow behaviors within pore–throat connections with different length-to-diameter ratios

(a) Piston-like displacement at the length-to-diameter ratio of 2.22.

(b) Snap-off at the length-to-diameter ratio of 3.44.

- Impacts of Snap-Off in porous media

The fluid dynamics inside the porous medium are then noticeably impacted by the snap-off event. These effects mainly include strong foam production, drainage–imbibition hysteresis, oil bridging effect, and unrecoverable oil droplet creation. The Bridging Effect of Oil [14]

I.6.4 Steam injection

Steam injection is a crucial enhanced oil recovery (EOR) method used to increase the extraction of heavy and viscous oils that are otherwise difficult to produce using conventional techniques. [5] Steam injection can take two basic forms: cyclic steam stimulation and steamflooding. Cyclic steaming is increasingly becoming the first phase in the development of a steamflood, which can yield oil recoveries approaching 80% of the initial oil in place, [6]

Cyclic Steam Stimulation (CSS), often referred to as the “huff and puff” method, involves three main stages: steam injection, soaking, and production. Steam Flooding involves continuous steam injection through dedicated injection wells, creating a steam front that pushes oil toward production wells. [5]

Conclusion

This chapter elucidates the complex dynamics of snap-off in porous media, underscoring its role as a primary mechanism for non-wetting phase trapping. Snap-off is governed by capillary dominance—specifically pore-throat geometry (length-to-diameter ratio $\geq \pi$), wettability, and interfacial tension—with imbibition processes exacerbating droplet fragmentation. The severity of trapping is dictated by both static petrophysical properties (porosity, saturation) and dynamic parameters (capillary number, viscosity ratio), which critically influence residual oil saturation. Steam injection effectively mitigates snap-off by reducing oil viscosity and interfacial tension, promoting droplet coalescence and mobility. These principles highlight the need for tailored recovery strategies addressing pore-scale heterogeneity, and future work should leverage advanced imaging and simulation tools to further decode snap-off mechanics, enabling more efficient hydrocarbon extraction in challenging reservoirs.



Chapter II

Experimental strategy and laboratory protocol

Introduction

This chapter details the experimental methodology employed to investigate multiphase flow dynamics and the snap-off phenomenon in a controlled porous medium. Utilizing a custom-designed mesofluidic system—a transparent PVC-based network emulating reservoir pore-throat structures this study systematically examines fluid displacement processes under varying conditions. Key oil properties (density, viscosity, interfacial tension) were characterized via precision instruments (Anton Paar SVM 3001 viscometer, Tensio CAD tensiometer), while wettability was quantified through contact angle measurements. Experimental procedures encompassed four core tests: drainage, imbibition and simultaneous injection and finally as a solution we chose steam injection to remove the snap off phenomenon.

II.1 Materials used

This section describes the material used in our: samples, fluids, tools and capillaries.

II.1.1 Brine

The brine used in all of the trials was created in the laboratory. To make this brine, dissolve 250g of NaCl in 1 liter of distilled water. This brine is utilized for the liquid/liquid displacements of the samples during the drainage and imbibitions tests.

II.1.2 Diesel

The diesel was used as oil in all monophasic and diphasic flow experiments, as well as imbibitions tests. The used diesel is sold by the company Naftal, whose characteristics are shown in the table (II.1).

Table II-1: Properties of the diesel used

Density at 15°C	0.828g/cm ³
Dynamic viscosity at 25 °C	3,45Cp
Surface tension at 20°C	30mN/m
Flash point	88°C
Pour point	-14°C
Initial boiling point	152°C
Final boiling point	320°C

Chromatography mass spectrometer which is a qualitative analytical for organic

compounds to elucidate the structure of species present even in small quantities in a sample. The oil analysis indicates that it's majorly composed of alkanes ranging from C10 to C20 contributing to its energy content, see Appendix A.

II.1.3 Crude oil

II.1.3.A Density and viscosity

- **Description of the Rotary viscometer:**

The Anton Paar SVM 3001 is a high-precision rotational Stabinger viscometer (figure) that we use for the simultaneous measurement of dynamic viscosity, kinematic viscosity, and density of liquids. This instrument employs a rotating U-tube with a magnetically driven rotor, where we determine viscosity by measuring the torque required to rotate the rotor within the test fluid, while density is measured concurrently using the oscillating U-tube principle. We primarily apply this advanced instrument for fuel testing—including diesel, gasoline, and jet fuel—as well as for comprehensive crude oil characterization, ensuring accurate and reliable fluid property data for our research and quality control processes.



Figure II.1: Rotary viscometer instrument

We start by making sure the instrument is clean, calibrated, and at the right temperature. (25 °) Then, we load the oil sample—either manually. Next, we set the measurement conditions like temperature (25°) and duration(2h). After that, we press “Start” to begin the test, and the system automatically measures viscosity, density, and temperature. Once done we can save the results.

II.1.3.B surface tension and interfacial tension

Description of Tensiometer

We utilize the TensioCAD analytical instrument to accurately measure surface tension

and interfacial tension (IFT) between immiscible phases, typically liquid/air or liquid/liquid systems, through high-precision force measurements. This tool is integral to our research for evaluating surfactant performance in reducing IFT between oil and water, as well as characterizing the stability of oil-water emulsions during production and separation processes. By providing reliable quantitative data, the TensioCAD enhances our understanding of fluid interactions and optimizes formulations for improved efficiency in enhanced oil recovery (EOR) and industrial separation applications.

we first pour the liquid (water and oil) sample into a clean container (30ml) and place it on the instrument's stage. Then, we lower the platinum plate into the liquid. The device measures the force as the plate interacts with the liquid surface. This force is then used to calculate the surface and interfacial tension. Finally, we view and analyze the results using the connected software. The following picture shows the stages of the experiment:



Figure II.2: Steps of measurement of surface and interfacial tension

II.1.4 Wettability determination

By measuring and comparing the contact angle between the glass plate and a water droplet and an oil droplet that have been carefully dispensed onto the substrate until they reach equilibrium, the imaging process is positioned perpendicularly to capture the side view of the droplet figure, and all experiments are conducted at laboratory temperature (25°).

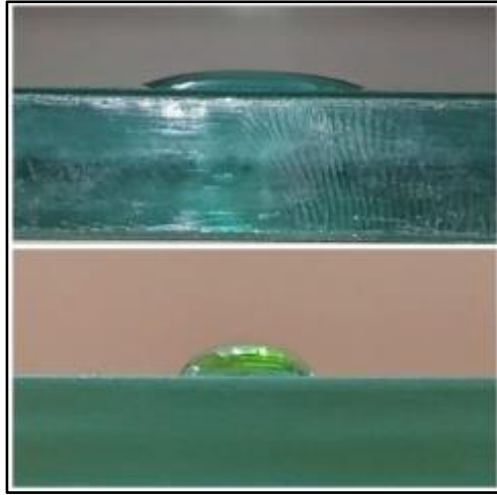


Figure II.3: Contact angle determination imaging

II.1.5 Description of the mesofluidic system

In our study we use a rectangular plate of pvc with dimensions (26/28 cm) which designate a network of pores (16 pores and 24 throat) each pore has a specific diameter between (1.85 / 1.52) shaped with a cylindrical form and throat with parallelepiped shape the distance between this later is about (4 / 5.25)

This practical model allow us to visualise realise a diphasique displacement in our case (water /oil) and the snap off phenomenon which is guaranteed with a preferential flow path in petroleum reservoir.

II.2 Experimental procedures:

We will do a series of experiments: drainage, imbibition, steam injection and simultaneous injection on the mesofluidic oil-wetting system, apparatus is shown in figure

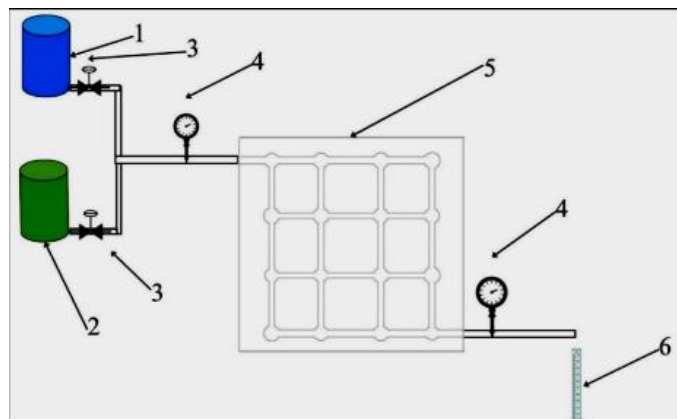


Figure II.4: Schematic representation of the mesofluidic system apparatus

(1) water injection reservoir, (2) Oil injection reservoir, (3) control valves, (4) manometers, (5) mesofluidic system, (6) graduated test tube.

II.2.1 Drainage

Step one:

Before starting the drainage experiment, we carefully prepare the mesofluidic system to ensure accurate and reproducible results. We begin by thoroughly cleaning the porous chip using a sequence of solvents, such as ethanol followed by distilled water, to eliminate any impurities that may affect wettability or flow behavior. After cleaning, we inspect all control valves, tubing, and connections for potential leaks. Ensuring a leak-free setup is essential for maintaining stable pressure conditions and preventing any fluid losses during the experiment.

Step two:

We open the oil reservoir valve and slowly inject oil into the system until the mesofluidic system is fully saturated (figure). We carefully monitor the injection process to ensure that the entire pore network is uniformly filled with oil, confirming visually that no air or water remains within the system.



Figure II.5: Saturation of the system with oil

Step three:

We start injecting water under specific initial pressure (0.0038 atm), adjusting the flow using the control valves and closely monitoring pressure changes on the manometers. We observe the progression of the water front as it displaces the oil within the mesofluidic

system. The displaced oil exits into the graduated test tube, and we record the collected volume at regular intervals for analysis.



Figure II.6: Preferential flow path results under $p=0.00387$



Figure II.7: Preferential flow path results under $p= 0.00775$ atm



Figure II.8: Preferential flow path results under $p= 0.01549$ atm



Figure II.9: Preferential flow path results under $p = 0.01936 \text{ atm}$

Step four:

We follow the preferential flow routes that emerge in the mesofluidic system and observe the displacement front and the trapped water (snap off phenomenon). To assess how well the displacement process works, we measure and record the amount of oil collected in the test tube at each pressure level.

Step five:

Once we observe that no further oil is being displaced, we stop the water injection, close all valves, and calculate the Recovery Factor.

$$\text{oil recovery}(\%) = \frac{V_{\text{produced oil}}}{V_{\text{initial oil in place}}} \times 100$$

We repeat the experiment several times and each time we change the pressure value as shown in figure

To assess how pressure affects the displacement dynamics and drainage process efficiency, we compare oil recovery rates under various injection pressures and along various flow pathways.

II.2.2 Imbibition :

Step one

First, we thoroughly clean the mesofluidic chip to remove any residual fluids or contaminants that could affect the experiment. Next, we saturate the system by injecting

water until the pores are completely filled, After saturation, we stabilize the system by allowing sufficient time for pressures to equilibrate across the apparatus, ensuring consistent initial conditions for the imbibition process.



Figure II.10: Saturation of the system with water

Step two:

we connect the water injection reservoir to the system, ensuring all fittings are secure to prevent leaks. Before initiating flow, we verify that all control valves are closed to maintain system integrity and avoid unintended fluid movement. Finally, we position the graduated test tube at the outlet to accurately collect and measure the volume of displaced water during the experiment.

Step three:

Inject oil slowly at a constant pressure (0,0034 atm) to displace water from the pore structure. Track the oil front movement through the mesofluidic network.

Observe, trapping (snap off) as shown in the figure, and bypassing of water due to unfavorable mobility and wettability.



Figure II.11: snap off phenomenon during imbibition proces

Step four:

We follow the preferential flow routes that emerge in the mesofluidic system and observe the displacement front. To assess how well the displacement process works, we measure and record the amount of water collected in the test tube at each pressure level.

Step five:

Water displaced by the oil is collected in the graduated test tube.

Record volume vs. time to calculate recovery.

water recovery(%)= $\frac{V_{\text{produced water}}}{V_{\text{initial water in place}}}$ $\times 100$
 water recovery%= $\frac{V_{\text{produced water}}}{V_{\text{initial water in place}}}$ $\times 100$

We repeat the experiment several times and each time we change the pressure value as shown in figure

Compare water recovery rates along different flow paths and under varying injection pressures to evaluate how pressure influences the displacement dynamics and efficiency of the imbibition process.

II.2.3 Simultaneous injection

1/ checking the full system from any leak or damage and gas bubbles

2/ we starting injection of oil and water at the same time and allow it to equilibrate for a few minutes

3/ starting increasing pressure progressively

4/observe the trapping (snap off)

5/ stop the injection when the system is full with fluid

The figure represents the result of this process:

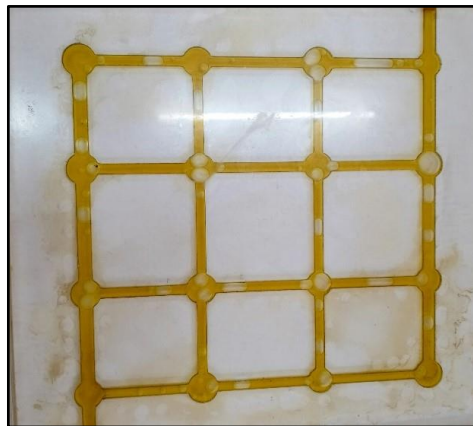


Figure II.12: simultaneous injection

The goal of this process is to create snap off phenomenon

II.3 Steam injection on PVC-mesofluidic system experiment

II.3.1 Description of the experiment

The experiment includes a setup for injecting steam into a mesofluidic PVC system placed on a core holder, observing its behavior, and collecting data on steam distribution. This set-up is designed to imitate conditions similar to those found in thermal enhanced oil recovery (TEOR) procedures and to aim to investigate the displacement of fluids in a porous medium.

The steam will be injected to the PVC- mesofluidic system under a temperature of 130 °C and an entry pressure of 2,7 atm the produced fluids will be collected in a graduated test tube to measure the volume under a range of different pressures bearings.

II.3.2 Material used on steam injection

- PVC – mesofluidic system: the previously used as the porous medium.
- Steam Source: a pressure cooker will serve as the steam source
- Steam Transfer System: temperature resistant silicon tubing to connect the pressure cooker to the system.
- Valves: to control the flow of steam.

- Thermometers: to monitor the temperature at various points.
- Pressure Gauges: to measure pressure within the system.
- Insulation Material: To insulate the tubing and maintain steam temperature.
- Core Holder: to hold the mesofluidic system, it should be placed in a stable, heat-resistant environment. (As shown in the image).
- Condenser: to cool and collect the steam after passing through the core holder, it should have an outlet leading to the collection graduated cylinder.
- Collection Graduated test tube: for measuring the volume of recovered liquids.

II.3.3 Experimental procedure

II.3.3.A Preparation of Equipment :

- after the mesofluidic system is 100% saturated with oil, water is injected into the system to displace the oil until only residual oil saturation remains. The pressure cooker is filled with water and ensured to be securely sealed, Connect and insulate a pipe to its release fitting direct the steam flow. A Polyester or heating tape (to maintain steam temperature and prevent heat loss).And bleeds are installed in the lines to remove any condensate.
- Securely connect appropriate silicon pipe lines from the pressure cooker to the inlet of the PVC-mesofluidic system to prevent any steam leakage, with bleeds to remove any condensate and wrap the silicone pipe and the core holder with polyester or heating tape to minimize heat loss and maintain the steam temperature.
- Attach another pipe or tube to the outlet of the PVC-mesofluidic system, directing it into a graduated test tube to collect and measure the displaced fluid.

II.3.3.B Steam Injection :

- Heat the pressure cooker until steam is generated. The steam should travel through the insulated pipe into the PVC-mesofluidic system, ensuring that it maintains its vapor phase.
- Monitor the steam flow to maintain consistent pressure.

II.3.3.C Fluid Displacement and Collection:

- As steam enters the PVC-mesofluidic system, it will displace the fluids within the mesofluidic channels.
- The displaced fluids will exit through the outlet pipe and be collected in the graduated test tube.

II.3.3.D Data recording and analysis:

- Measure the volume of displaced fluid accurately.
- Measure the oil recovery rate.

- Measure the transferred heat energy Q by equation (II-7).
- Record Observations in flow behavior through pores.
- Compare the collected data previous experiment results to evaluate the efficiency and characteristics of steam displacement in the mesofluidic system.

Note:

All the previous steps were carried out under three different values of temperature (60 °C, 65 °C, 70°C).

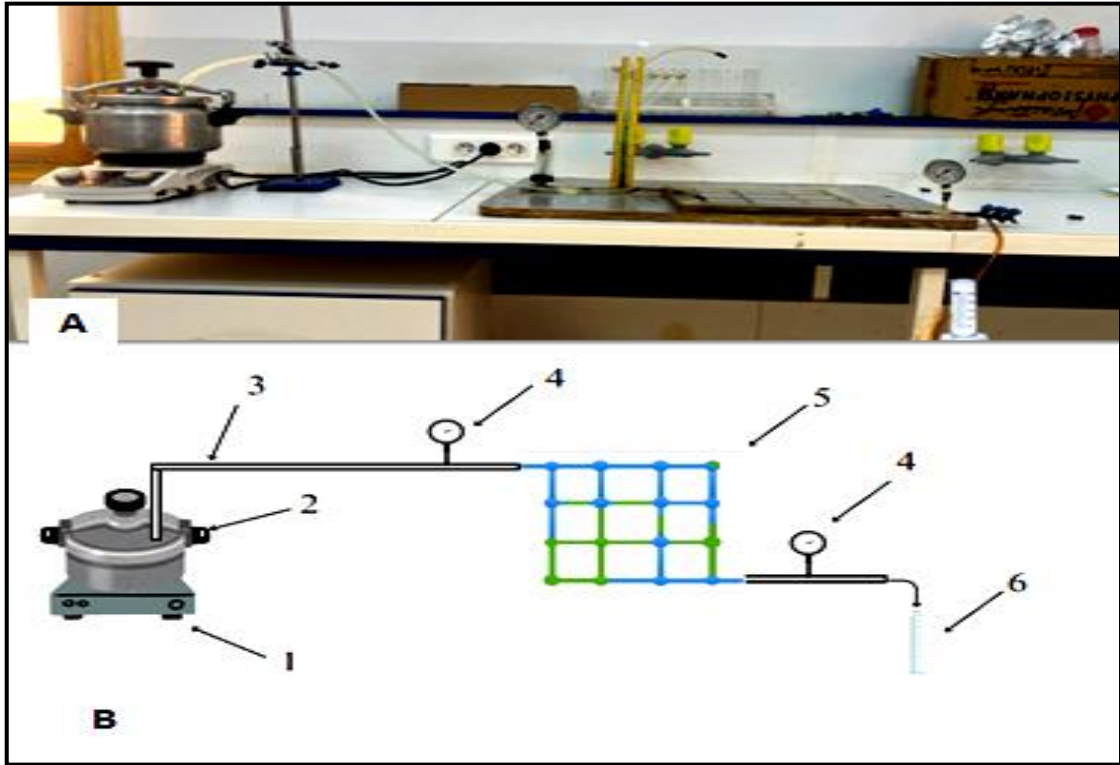


Figure II.13: A) Steam injection experiment installation B) Schematic representation of the Steam injection installation

- (1) heat-source (2) pressure cooker (3) silicon tube (4) manometers (5) PVC-mesofluidic system (6) graduted test tube.

Conclusion:

In this chapter, we have carefully examined all of the available resources and methods. for modeling and characterizing the water-oil flow dynamics in two phases in porous Media (drainage,imbibition, simultanues injection),we found that This study conclusively demonstrates that the snap-off phenomenon—a critical pore-scale trapping mechanism driven by capillary instabilities—significantly impedes hydrocarbon recovery by fragmenting non-wetting phases into isolated, immobile ganglia within narrow pore throats. The experimental framework reveals that snap-off is amplified under imbibition-dominated

flow regimes and in geometries where pore-throat length-to-diameter ratios exceed critical thresholds ($\geq \pi$), exacerbating residual saturation.

steam injection, emerge as a potent solution to mitigate snap-off. By elevating temperature, steam simultaneously reduces oil viscosity and interfacial tension, destabilizing capillary forces that sustain trapped droplets. This dual action promotes droplet coalescence and remobilization, transforming disconnected ganglia into continuous, recoverable flow paths.



Chapter III

Results and discussion

Table III-1: oil parameter

Parameter	Value	Unit
Temperature	25	°C
Dynamic Viscosity	152.85	mPa·s
Kinematic Viscosity	185.32	mm ² /s
Volumetric Mass (Density)	0.847	g/cm ³

The tensiometer as a result give us graph displays a force (weight) versus time curves shown in the figure:

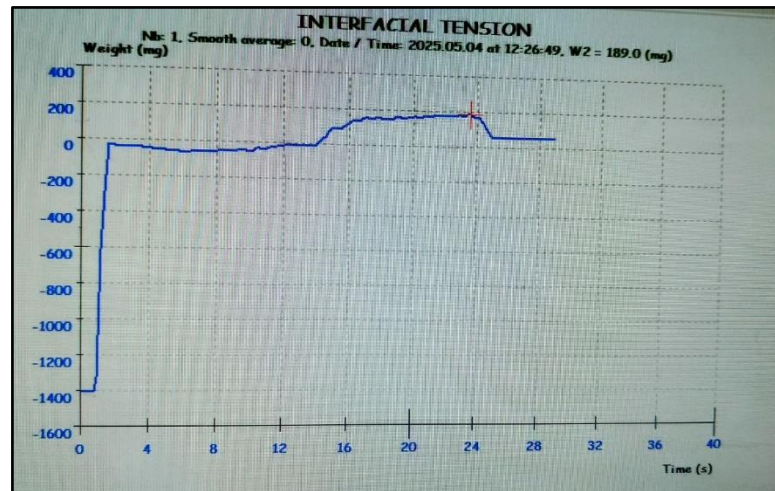


Figure III.2: graph displays a force (weight) versus time curves

The program gives us directly the result of superficial tension

Superficial tension = 32.5(mN/m)

To calculate the superficial tension, we use the formula

$$\delta = \frac{m \cdot g}{2 \times (l \times e)} \quad (\text{III};22)$$

We found that:

Interfacial tension = 0.024 (N/m)

III.2 Contact angle measurements results:

The glass plate's wettability characteristics are revealed by the results of the contact angle measurements. The oil contact angle at the oil/glass plate interface (A) was 110°, demonstrating the glass plate oleophobic and non-wetting properties. On the other hand, a contact angle of 10° was found (B), indicating beneficial wetting behavior and a plate surface that is hydrophile.

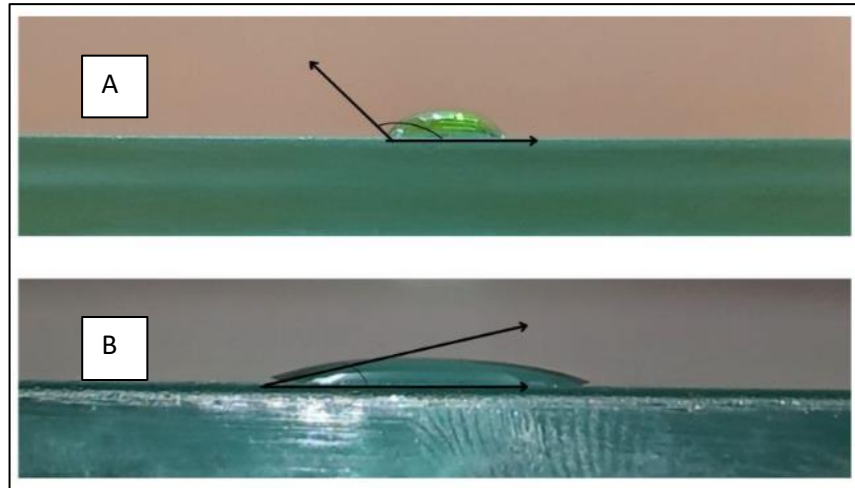


Figure III.3: Contact angle between: (A) oil drop and glass plate (B) water drop and glass plate

III.3 Preferential flow path during drainage process on mesofluidic system results

Figures illustrate the various oil/water displacement paths that are seen at various pressure ranges at drainage process. Additionally, the recovered oil was calculated (Table III.3).

Table III-2: Oil recovery results

Differential pressure (atm)	Recovered oil volume (ml)	Trapped oil volume (ml)	Recovery factor (%)
0.003872687	33	13	0,71
0.007745374	25	21	0,54
0.01161806	26	20	0,56
0.01549075	22	24	0,47
0.01936343	20	26	0,54

The experiment investigates the behavior of oil displacement under varying differential pressures, with a focus on the volumes of recovered and trapped oil, as well as the corresponding recovery factor. The objective is to understand the effect of pressure on displacement efficiency.

At low differential pressure (0.00387 atm), the recovery factor is highest (71%).

- This suggests that under capillary-dominated flow, displacement is stable and more efficient.
- The displacement front moves uniformly, allowing a larger portion of the oil to be mobilized and produced.

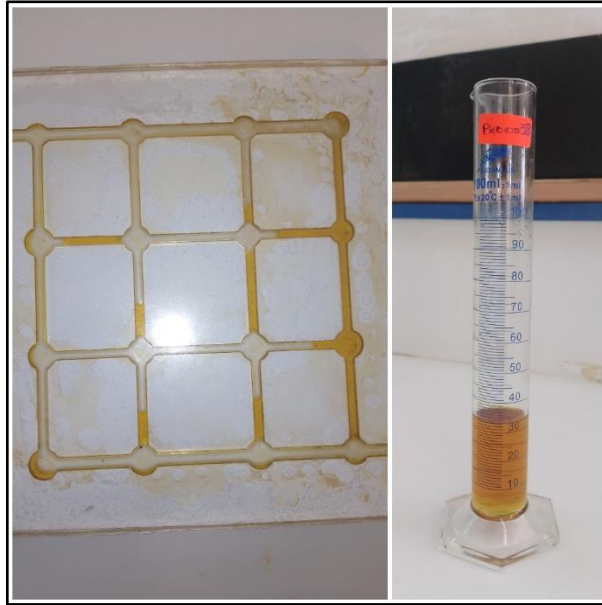


Figure III.4: Preferential flow path results and Recovered oil under $p=0.00387$

As the pressure increases to 0.00775 – 0.01549 atm, the recovery factor decreases (down to ~47%).

-This is likely due to the onset of viscous fingering, where the displacing fluid bypasses oil pockets, leading to poor sweep efficiency and higher residual oil saturation.

-High flow rates associated with increased pressure gradients may cause instabilities in the displacement front.



Figure III.5 : Preferential flow path results and Recovered oil under $p= 0.00775$ atm

Preferential flow path results and Recovered oil under $p= 0.00775$ atm

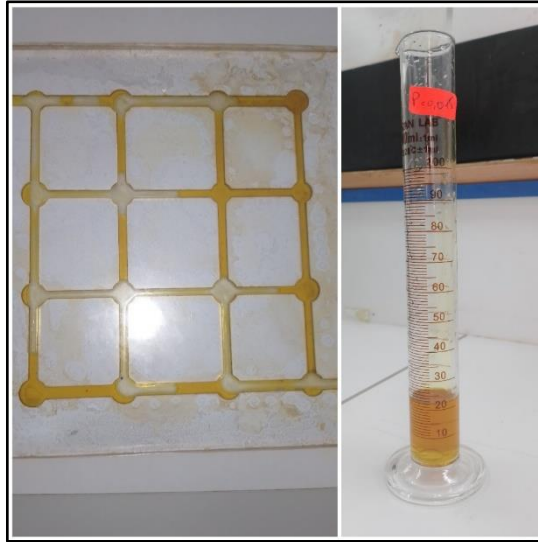


Figure III.6: Preferential flow path results and Recoverd oil under $p= 0.01549$ atm

At 0.01936 atm, the recovery factor is listed as 54%, but calculated value (~43.5%) indicates further efficiency loss

_The higher differential pressure does not guarantee improved recovery. Instead, it may exacerbate fingering or channeling, leaving behind more trapped oil.

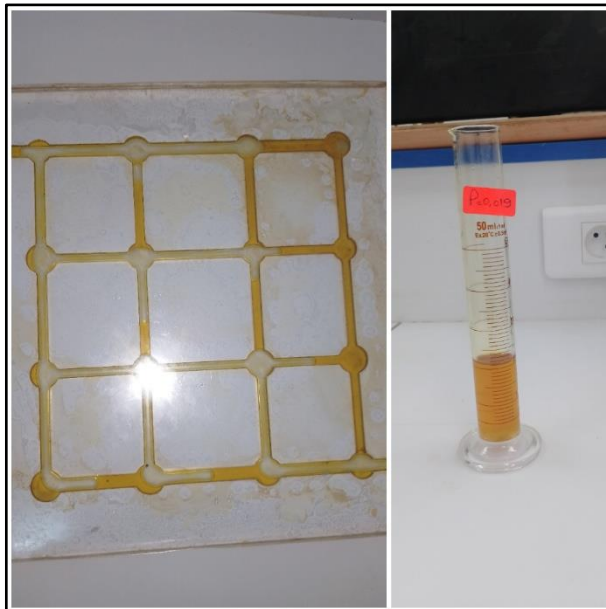


Figure III.7: Preferential flow path results and Recoverd oil under $p= 0.01936$ atm

Preferential flow path results and Recovered oil under $p= 0.01936$ atm

As the differential pressure increases, the trapped oil volume rises from 13 ml to 26 ml, indicating that the displacement process becomes less effective at higher pressures. This trend is likely attributed to a combination of capillary end effects, pore-scale bypassing, and increased dominance of viscous forces, all of which contribute to greater residual oil saturation. At low differential pressures, capillary forces prevail, resulting in a more uniform and piston-like displacement front that enhances sweep efficiency. However, as pressure increases, viscous forces begin to dominate, leading to unstable displacement characterized by fingering and channeling, particularly when the mobility ratio is unfavorable—such as when a low-viscosity displacing fluid attempts to push a more viscous oil. This imbalance reduces the effectiveness of oil recovery despite higher applied pressures.

III.4 Snap off during imbibition process

The table below give us recovered water volume and Recovery factor at various pressure ranges at imbibition process:

Table III-3: water recovery results

Differential pressure (atm)	Recovered water volume (ml)	Trapped water volume (ml)	Recovery factor (%)
0,00346605	45	1	0,978
0,00693211	42	4	0,913
0,01039816	43	3	0,93
0,01386422	43	3	0,93
0,01733027	44	2	0,95

High recovery factors (>91%) are observed across all pressure ranges, indicating an efficient imbibition process.

The process is dominated by capillary-driven snap-off, especially under oil-wet conditions where the invading water preferentially occupies smaller pores and corners.

Snap-off in this context refers to the pinching-off of non-wetting phase by advancing wetting-phase menisci in constricted pore throats, leading to effective displacement.

The figure bellow represents the snap off phenomenon

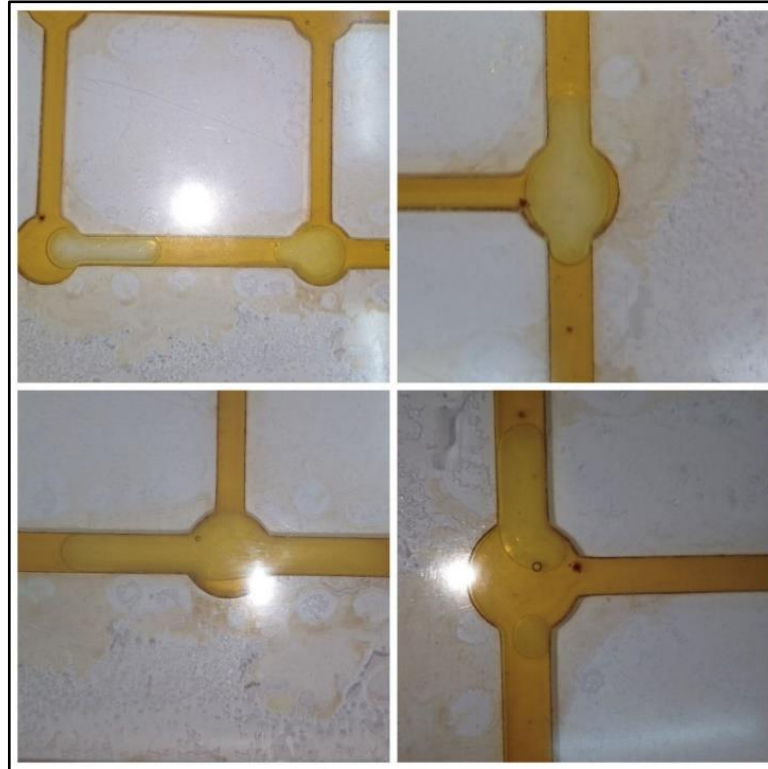


Figure III.8: snap off phenomenon during imbibition proces

snap off phenomenon during imbibition proces

We notice that snap off phenomenon appear in the smal pores particularly in narrow pore throats and bloc the displacement of the oil for a period

The efficiency of this process depends on Pore structure (mesofluidic geometry), Interfacial tension, Contact angle (oil-wetness) and Pressure gradient (ΔP). At low pressure gradients, capillary action dominates, promoting snap-off and minimizing viscous bypassing. At higher pressures, although recovery remains high, a slight shift toward viscous-dominated flow may reduce snap-off frequency, causing slightly more trapped water.

III.5 Simultaneous injection

During simultaneous oil-water injection in the oil-wet microfluidic system, water (non-wetting phase) undergoes snap-off due to three synergistic mechanisms:

-Geometric Trigger: Throats with high length-to-diameter ratios act as capillary valves, where abrupt diameter changes amplify interfacial curvature differences

-Capillary Dominance: Advancing oil (wetting phase) surrounds water threads, causing capillary pressure to exceed viscous forces and pinch off water into isolated droplets

-Dynamic

Instability: Rapid pressure increases intensify fluid interference, creating unstable water-oil interfaces that fragment preferentially in throats.



Figure III.9: snap off phenomenon during simultaneous injection

III.6 Visualization of Snap-off phenomenon

The following figures describe the mechanism and process of occurrence of the Snap-off phenomenon:

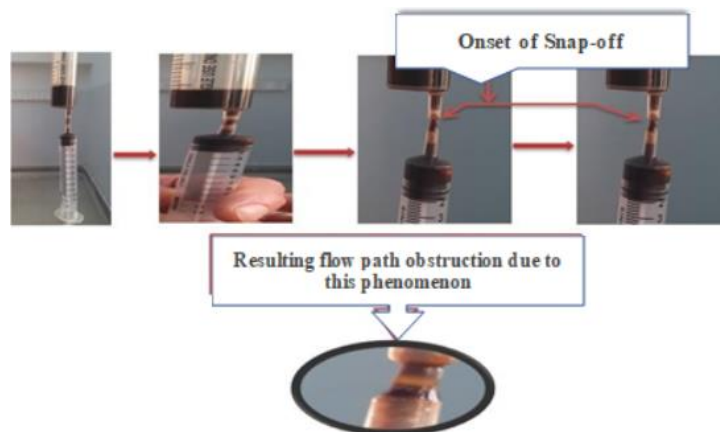


Figure III.10: Photographs showing the occurrence of Snap-off phenomena.

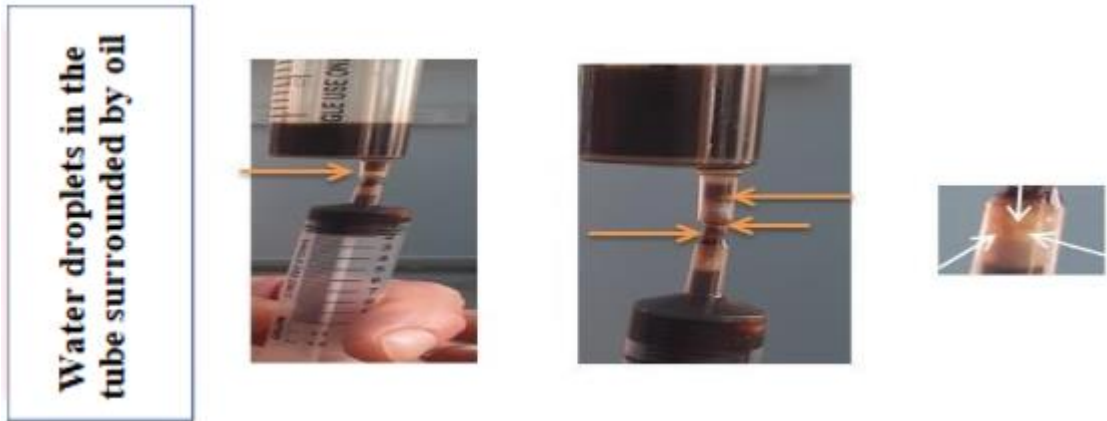


Figure III.11: Dispersion of water droplets in oil

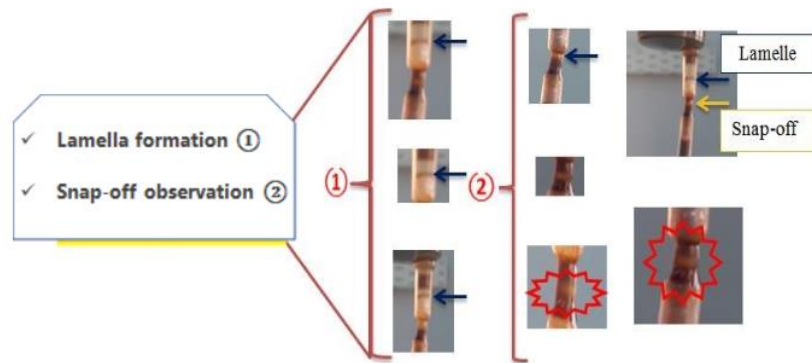


Figure III.12: Lamella formation and water droplet trapping

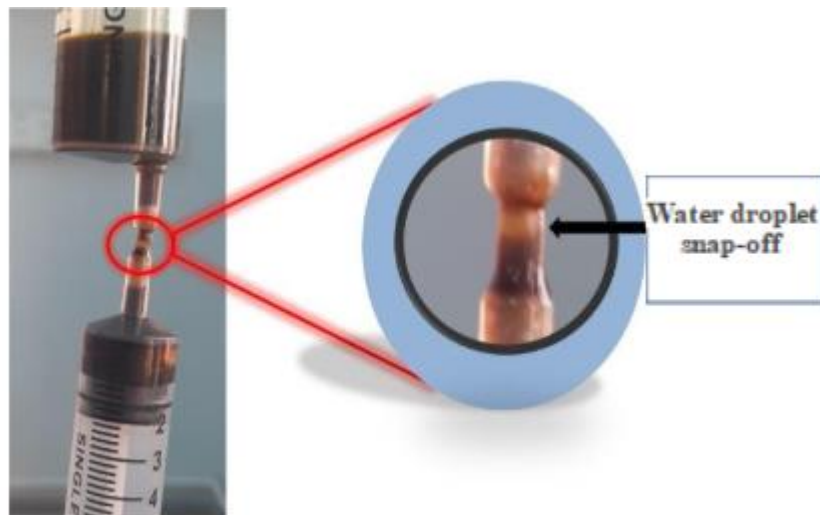


Figure III.13: Snap-off of a non-wetting phase droplet



Figure III.14: Formation of a film around the inner surface

III.6.1 Observation and interpretation

_ Water does not invade unless the pressure exceeds the “threshold” inlet pressure, and is the reason for effluent blockage, despite the fact that a vacuum was imposed on the 1st time, but flow was still impossible.

- The ratio of film thickness to capillary radius “h/R” prior to initiation of the experiment is equal to “1”, since the capillary is oleophilic. It is therefore full of the wetting part, after which it will decrease under the effect of a depression in the presence of two phases until it reaches a constant value.

- Snap-off occurs during drainage processes.

- The snap-off phenomenon produces a “film” of the wetting phase separating the non-wetting phase, after which it disappears.

III.6.2 Numerical application

The Snap-off phenomenon is characterized and described by certain parameters, among which parameters can be calculated as follows:

1/Capillary pressure "in the small diameter

$$P_c = \frac{2\sigma}{r} = \frac{2 \times 5 \times 0.001}{0.5 \times 0.001} = 20 Pa \quad (\text{III};23)$$

2/Snap-off time “ τ_s ”

$$\tau_s = \frac{\mu \sigma r}{\sigma} = \frac{0.3 \times 0.5 \times 10^{-5}}{5 \times 10^{-3}} = 3 \times 10^{-4} \quad (\text{III};24)$$

3/Time break-up « t_b »

This is an important parameter as it affects the size of the bubbles generated and the flow properties of the bubble through the porous medium. It is measured experimentally as the time between the bubble front passing the constriction until the small “snap-off” bubbles detach and block the pore.

By applying Vegas Pro 11.0 (see figure) we can slow down the experiment and measure the break-up time more accurately.

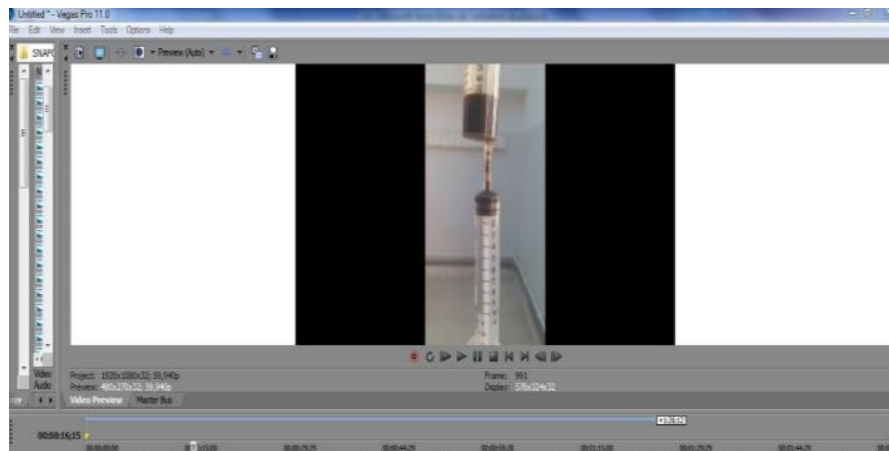


Figure III.15: Observation of Snap-off phenomena using Vegas Pro 11.0.

By observation we hold t_b [0 :51 :19-0 :51 :93], so $t_b = 0.74$ s

$$\tau_b = \frac{t_b}{3 \times \tau_s} = \frac{0.74}{3 \times 3 \times 10^{-4}} = 822.2 \quad (\text{III};25)+$$

III.7 Steam injection on mesofluidic system results

To calculate the heat energy transferred of the PVC-mesofluidic system, we need to take into account the volume of system, volumetric heat capacity of system and temperature difference between the injected steam and the reservoir. Results are shown in table (IV.16)

Table III-4: Heat energy transferred results.

Test	Temperature (°C)	Heat energy transferred (Joule)
01	60	92,181
02	65	85,597
03	70	79,013

To determine the amount of residual oil recovered by steam injection (Table III-5), we need to calculate the thermal efficiency and consider the conditions provided. Given that the residual oil volume after primary recovery is 25,901 ml and knowing the steam and system temperatures, we can proceed with an estimation.

Table III-5: Residual oil recovered by steam injection's temperature ranges

Differential temperature (°C)	Recovery factor (%)	Volume of residual oil recovered by steam injection (ml)
60	25	6,47525
65	30	7,7703
70	50	12,9505

The table demonstrates that the efficiency of steam injection on mesofluidic system for residual oil recovery increases with increasing differential temperatures. At 60°C, the lowest recovery factor of 25% corresponds to a recovered residual oil volume of 6,47525 ml. When differential temperature increases to 65°C, the recovery factor increases to 30%, with a corresponding residual oil volume of 7,7703 ml. Further increasing differential temperature to 70°C results in the highest recovery factor of 50% and a residual oil volume of 12,9505 ml. These results indicate that high differential temperatures are more effective for maximizing both the recovery factor and the volume of residual oil recovered according to volumetric heat capacity of mesofluidic system.

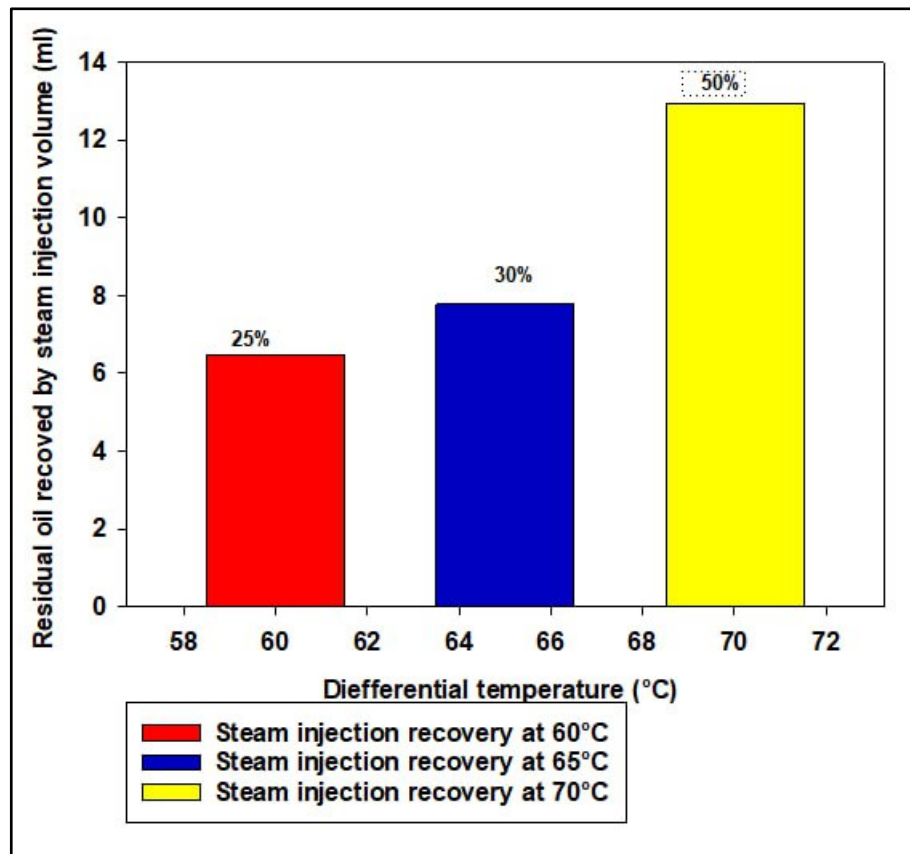
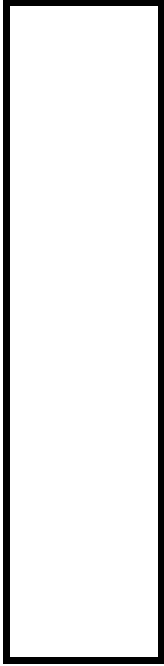


Figure III.16: Residual oil recovered by steam injection in function of mesofluidic system temperature.

Conclusion:

Impact of snap off: The study confirmed that pore size and distribution significantly influence fluid flow dynamics. Larger pores enhance oil recovery by providing continuous pathways for fluid flow, whereas smaller pores can trap water and impede overall flow. This insight underscores the importance of characterizing pore structures in reservoir rocks to optimize oil recovery strategies.

Effectiveness of Heat-Based Recovery Techniques: Heat-based recovery methods, such as steam injection, were observed to improve oil displacement efficiency. However, their effectiveness was highly dependent on the specific pore structure of the reservoir. This finding suggests that the success of thermal recovery methods can vary widely and should be tailored to the reservoir's geological characteristics.



Conclusion and recommendation

General Conclusion and Recommendations

This study's objectives were to model and describe the displacement of two-phase flow in porous media and investigate the impact of snap off on

recovery of oil. The study sought to address a number of important questions:

What effect do oil recovery and drainage fluid channels have?

-What is the impact of drainage fluid pathways and oil recovery?

-How does affect the snap off durring imbibition process?

-How effective are different heat-based oil recovery techniques?

The literature review underscored the importance of understanding fluid flow dynamics in heterogeneous porous media, the impact of snap off in oil recovery, .

Conducted experiments successfully demonstrated the potential of mesofluidic systems to replicate oil-wet porous media and visualize multiphase flow behavior at the pore scale. The transparent structure enabled direct observation of snap-off events during drainage, imbibition, and simultaneous injection processes.

During drainage, low-pressure injection favored piston-like displacement and yielded higher oil recovery (up to 71%). However, increasing pressure induced viscous fingering and increased residual oil. In contrast, imbibition benefited from snap-off of the displaced phase, yielding recovery factors above 91% across various pressures.

Co-injection experiments revealed dynamic instability and frequent snap-off events of the non-wetting phase. These were governed by throat geometry and interfacial interactions, resulting in dispersed droplets and irregular flow pathways

Steam injection proved effective in remobilizing trapped oil. Increasing the steam temperature from 60°C to 70°C improved recovery from 25% to 50%. The heat reduced oil viscosity and interfacial tension, mitigating the snap-off effect and restoring flow continuity.

Experimental results confirm that pore geometry (throat-pore ratio) and surface wettability critically affect snap-off behavior. The mesofluidic model's oil-wet conditions amplified capillary trapping, underlining the importance of reservoir-specific characterization.

Recommendations

Advanced Mesofluidic Imaging: Utilize mesofluidic devices to visualize and quantify multiphase flow behavior. This approach is recommended for better understanding fluid interactions at the pore scale and optimizing recovery strategies.

Conclusion and Recommendations

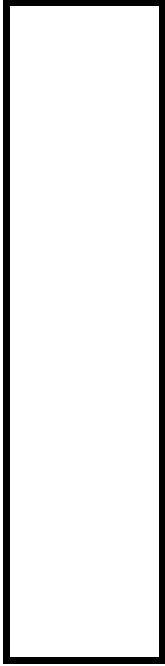
Pressure-Controlled Injection: Maintain low differential pressures during water injection in oil-wet systems to avoid viscous fingering and improve sweep efficiency during drainage processes.

Utilize Imbibition in Oil-Wet Conditions: Favor imbibition processes when the reservoir is strongly oil-wet, as the capillary-driven snap-off enhances recovery by displacing the non-wetting phase effectively.

Thermal Recovery Implementation: Apply steam injection in reservoirs with known snap-off challenges. Elevated temperatures help reduce capillary trapping, improve mobility, and increase oil displacement efficiency.

Comprehensive Petrophysical Characterization: Prioritize pore-scale geometry and wettability analysis in reservoir studies to predict flow behavior and optimize enhanced oil recovery (EOR) methods.

Model Validation and Simulation Coupling: Combine mesofluidic observations with numerical modeling to build predictive tools that better represent the dynamics of flow in oil-wet reservoirs.



References

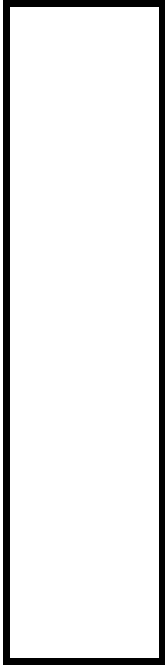
References

References

1. alamooti, A.malekabadi,F. science direct .com. [En ligne] 2022. <https://www.sciencedirect.com/topics/engineering/relative-permeability>.
2. ghulam, A.iqbal. science direct .com. [En ligne] 2016. (<https://www.sciencedirect.com/topics/engineering/effective-permeability>).
3. nasiru, l,m . bashirul h. science direct. *energy reports*. [En ligne] 2022. <https://www.sciencedirect.com/topics/engineering/salt-cavern>.
4. Ganat, T . Badawy,A. *Rock Properties and Reservoir Engineering: A Practical View*. Cairo, Egypt : Springer Nature Switzerland AG, 2022.
5. tarek, a. *Reservoir Engineering*. 50 Hampshire Street, 5th Floor, Cambridge, MA 02139, United States : Gulf Professional Publishing, 2019.
6. Yao, J.Guihe,L. researchGate. [En ligne] 2023. https://www.researchgate.net/figure/Relationship-between-the-capillary-number-and-snap-off-time-using-the-BD-model-a_fig4_375729757.
7. ghulam, satter and. predico. [En ligne] 2016. <https://predico.scrollhelp.site/afaum/fluid-saturations>.
8. Djebbar, T . Erle c . D. *Petrophysics Theory and Practice of Measuring Reservoir Rock and Fluid Transport Properties*. 225 Wyman Street, Waltham, MA 02451, USA : Gulf Professional Publishing, First edition 1996.Fourth edition 2015.
9. Dandekar, Abhijit Y. *Petroleum Reservoir Rock and Fluid Properties*. London New York Petroleum : Taylor & Francis Group, 2013.
10. Apostolos, K. perminc tipm laboratory. [En ligne] (<https://perminc.com/resources/fundamentals-of-fluid-flow-in-porous-media/chapter-2-the-porous-medium/multi-phase-saturated-rock-properties/phase-trapping/bypassing/>).
11. Marle.ch. *multiphase flow in porous media*. paris : technip, 1981.
12. blunt, M. *multiphase flow in permiable media a pore scale perspective*. cambridge : cambridge university press, 2017.
13. Guihe li, jia yao. MPDI. [En ligne] 2023. (<https://www.mdpi.com/2673-4117/4/4/163>).
14. Guihe, li . jia .gia ,yao. mdpi. [En ligne] 2023. (<https://www.mdpi.com/2673-4117/4/4/163>).
15. kruss scientific. [En ligne] (<https://www.kruss-scientific.com/en/know-how/glossary/interfacial-tension>).

References

16. pallab.gh. interfacial tension. [En ligne] <http://kinampark.com/PL/files/Ghosh%2C%20Interfacial%20Tension.pdf>.
17. Innova by nakasawa. [En ligne] 2024. <https://innovamas.nakasawaresources.com/en/steam-injection-techniques/>.
18. E, okandan. *heavy crude oil recovery*. s.l. : MrtinusNijhoff, 1984.
19. kantzias, A.bryan,J.taheri,S. *fundamentals of fluid flow in porous media* .
20. WHEATON, R. *FUNDAMENTALS OF APPLIED RESERVOIR ENGINEERING Appraisal, Economics,and Optimization*. 50 Hampshire Street, 5th Floor, Cambridge, MA 02139, USA : Gulf Professional Publishing, 2016.
21. Almohammad, farah N . faculty.uobasrah. [En ligne] https://www.google.com/url?sa=t&source=web&rct=j&opi=89978449&url=https://faculty.uobasrah.edu.iq/uploads/teaching/1702065787.pdf&ved=2ahUKEwiunJWq67SNAX9UqQEHXp0OLsQFnoECCcQAQ&sqi=2&usg=AOvVaw1uQrVj_CnuLGd7EChIND69.
22. z, ADJOU . *Etude des écoulements multiphasiques dans les capillaires à mouillabilité mixte*. ouargla : Université Kasdi Merbah-Ouargla, 2024.
23. Pierre, D. *ESSENTIALS OF reservoir engineering*. 27 rue Ginoux, 75737 PARIS Cedex 15, FRANCE : Editions TECHNIP, 2007.
24. NONO, F. *Caractérisation polyphasique de la zone de transition dans un réservoir pétrolier carbonaté*. Centre de Bordeaux : l'École Nationale Supérieure d'Arts et Métiers, 2014.
25. *Basics of Reservoir Engineering –Module I*. 2008.
26. AGU. <https://agupubs.onlinelibrary.wiley.com/doi/full/10.1029/2020WR029476>. [En ligne] 2021.

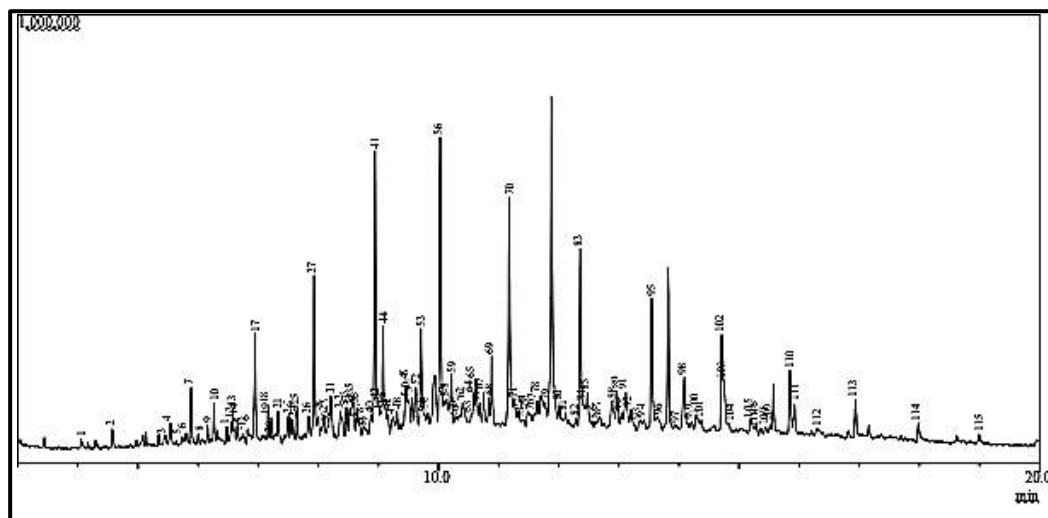


Appendix

APPENDIX

Appendix A

Diesel chromatographmass spectrometry analysis report



Peak	Area%	Similarity	Index Name
1	0.20	96	767 Heptane, 2-methyl-
2	0.38	93	800 Octane
7	0.92	94	900 Nonane
11	0.32	90	956 1-Octanol, 2-butyl-
12	0.41	95	963 Nonane, 4-methyl-
16	0.30	90	989 Cyclohexane, 1-methyl-2-propyl-
17	2.26	93	1001 Decane
18	0.44	93	1023 Heptane, 3,3,5-trimethyl-
24	0.32	93	1065 Decane, 2-methyl-
27	2.82	97	1101 Undecane
32	1.07	92	1144 Cyclohexane, pentyl-
33	0.68	92	1154 Undecane, 2,5-dimethyl-
35	1.41	93	1164 Dodecane, 2-methyl-
36	0.53	91	1171 Undecane, 3-methyl-
41	5.26	96	1201 Dodecane
44	2.01	94	1213 Undecane, 4,6-dimethyl-
48	0.52	90	1235 Cyclohexane, 2-butyl-1,1,3-trimethyl-
52	1.17	94	1264 Dodecane, 2-methyl-
53	2.46	94	1272 Dodecane, 4,6-dimethyl-
56	6.36	96	1301 Tetradecane

Appendix

67	0.90	92	1364	Heptadecane
69	1.49	92	1376	Dodecane, 2,6,10-trimethyl-
70	5.56	96	1401	Tetradecane
77	0.70	95	1441	Naphthalene, 1,3-dimethyl-
83	3.78	97	1501	Heptadecane
85	1.18	92	1511	Butylated Hydroxytoluene
95	3.21	97	1602	Heptadecane
98	1.64	93	1648	Octadecane
02	2.23	96	1702	Heptadecane
05	0.55	91	1745	Eicosane
10	1.42	96	1803	Heneicosane
11	0.79	92	1810	Eicosane
13	0.87	96	1903	Eicosane
14	0.41	95	2003	Eicosane
15	0.23	92	2104	Eicosane